Spring 3-13-2019

The Role of Specific Integrase Strand Transfer Inhibitors (INSTIs) in the Alteration of Oligodendrocyte Maturation and Myelination in Hand

Bassam N. Zidane
University of Pennsylvania, bzidane@dental.upenn.edu

Follow this and additional works at: https://repository.upenn.edu/dental_theses

Part of the Dentistry Commons, and the Neurology Commons

The Role of Specific Integrase Strand Transfer Inhibitors (INSTIs) in the Alteration of Oligodendrocyte Maturation and Myelination in Hand

Abstract

Currently, thirty-seven million people are infected with human immunodeficiency virus-1 (HIV-1) worldwide. Thankfully, the development of combined antiretroviral therapy (cART) regimens has decreased mortality and significantly improved the overall quality of life for these patients. However, approximately half of all patients clinically manifest with HIV-associated neurocognitive disorder (HAND), a spectrum of cognitive, motor, and behavioral abnormalities which histologically present as non-specific gliosis, synaptodendritc damage and loss of white matter and myelin. Furthermore, the severity of white matter damage correlates with the length of ART duration. However, almost no studies have been performed to determine how the myelin sheath or the oligodendrocytes that synthesize the sheath are damaged. Thus, we hypothesized that the administration of ART contributed in part to the myelin loss in the CNS of HIV-positive patients. Previously, we have reported that the protease inhibitor class of ART drugs hampered the *in vitro* differentiation of oligodendrocytes. Given that the new US guidelines for treating HIV patients recommends a new class of drugs, the *integrase* strand transfer *inhibitors* (INSTIs) as front-line therapy, we examined if two specific INSTIs, Elvitegravir (EVG) and raltegravir (RAL), altered the survival and/or maturation of developing oligodendrocytes *in vitro* and *in vivo*. We found that treatment of oligodendrocyte precursor cells (OPCs) with EVG, but not RAL, during differentiation reduced the number of cells positive for immature oligodendrocyte marker galactosylceramide (GalC) and mature oligodendrocyte marker myelin basic protein (MBP) *in vitro*, as well as the synthesis of myelin proteins. However, neither EVG or RAL induced cell loss or apoptosis, as determined by cell counts and TUNEL assays, suggesting that EVG does not affect OPC viability but instead, inhibits differentiation. EVG-induced oligodendrocyte differentiation deficits could be reversed by pre-treating the cells with a drug that pharmacologically inhibits the phosphorylation of eukaryotic initiation factor 2α (eIF2α) through the cellular integrated stress response (ISR). Finally, *in vivo,* mice receiving EVG/COBI failed to remyelinate the corpus callosum during the three week recovery period following demyelination, after cuprizone treatment. Although EVG/COBI treatment by itself did not cause overt white matter loss in this brain region. Our study demonstrates that EVG, but not RAL, inhibits oligodendrocyte precursor cell differentiation both *in vitro* and *in vivo*. Furthermore, EVG may be inhibiting oligodendrocyte precursor cell differentiation though activation of the ISR. Also, we found that the effects of EVG on oligodendrocyte differentiation could be attenuated *in vitro* by inhibiting the ISR. These studies suggest that ART may contribute to cognitive impairment by inhibiting renewal and replacement of oligodendrocytes in adults or development of oligodendrocytes in children. Further, our results suggest an ISR inhibitor might attenuate the negative effect of EVG on the maturation of oligodendrocytes. Our findings also suggest that development of less toxic ART compounds and adjunctive therapies are needed to minimize the side effects of ART on the CNS.

Degree Type
Thesis

Degree Name
DScD (Doctor of Science in Dentistry)

University of Pennsylvania Dental Medicine

THESIS

Presented to the Faculty of Penn Dental Medicine in Fulfillment of the Requirements for the Degree of Doctor of Science in Dentistry

_____ _____

_____ _____

THE ROLE OF SPECIFIC INTEGRASE STRAND TRANSFER INHIBITORS (INSTIs) IN THE ALTERATION OF OLIGODENDROCYTE MATURATION AND MYELINATION IN HAND

Bassam N. Zidane

University of Pennsylvania; bzidane@kau.sa.edu

In

Doctorate of Science in Dentistry Program

Presented to the Faculty of the University of Pennsylvania

In

Partial Fulfillment of the Requirements for the

Degree of Doctorate of Science in Dentistry - Spring 2019

Supervisor of Dissertation

Signature:_____

Typed Name

Full Faculty Title

Co-Supervisor of Dissertation

Signature:_____

Typed Name

Full Faculty Title

Graduate Group Chairperson

Signature_____

Typed Name

Full faculty title

Dissertation Committee *(Typed Names and faculty titles; no signatures necessary)*

_____

_____

_____

TABLE OF CONTENTS

ABSTRACT:

Currently, thirty-seven million people are infected with human immunodeficiency virus-1 (HIV-1) worldwide. Thankfully, the development of combined antiretroviral therapy (cART) regimens has decreased mortality and significantly improved the overall quality of life for these patients. However, approximately half of all patients clinically manifest with HIV-associated neurocognitive disorder (HAND), a spectrum of cognitive, motor, and behavioral abnormalities which histologically present as non-specific gliosis, synaptodendritc damage and loss of white matter and myelin. Furthermore, the severity of white matter damage correlates with the length of ART duration. However, almost no studies have been performed to determine how the myelin sheath or the oligodendrocytes that synthesize the sheath are damaged. Thus, we hypothesized that the administration of ART contributed in part to the myelin loss in the CNS of HIV-positive patients. Previously, we have reported that the protease inhibitor class of ART drugs hampered the *in vitro* differentiation of oligodendrocytes. Given that the new US guidelines for treating HIV patients recommends a new class of drugs, the integrase strand transfer inhibitors (INSTIs) as front-line therapy, we examined if two specific INSTIs, Elvitegravir (EVG) and raltegravir (RAL), altered the survival and/or maturation of developing oligodendrocytes *in vitro* and *in vivo*. We found that treatment of oligodendrocyte precursor cells (OPCs) with EVG, but not RAL, during differentiation reduced the number of cells positive for immature oligodendrocyte marker galactosylceramide (GalC) and mature oligodendrocyte marker myelin basic protein (MBP) *in vitro*, as well as the synthesis of myelin proteins. However, neither EVG or RAL induced cell loss

7

or apoptosis, as determined by cell counts and TUNEL assays, suggesting that EVG does not affect OPC viability but instead, inhibits differentiation. EVG-induced oligodendrocyte differentiation deficits could be reversed by pre-treating the cells with a drug that pharmacologically inhibits the phosphorylation of eukaryotic initiation factor 2 α (eIF2α) through the cellular integrated stress response (ISR). Finally, *in vivo,* mice receiving EVG/COBI failed to remyelinate the corpus callosum during the three week recovery period following demyelination, after cuprizone treatment. Although EVG/COBI treatment by itself did not cause overt white matter loss in this brain region. Our study demonstrates that EVG, but not RAL, inhibits oligodendrocyte precursor cell differentiation both *in vitro* and *in vivo.* Furthermore, EVG may be inhibiting oligodendrocyte precursor cell differentiation though activation of the ISR. Also, we found that the effects of EVG on oligodendrocyte differentiation could be attenuated *in vitro* by inhibiting the ISR. These studies suggest that ART may contribute to cognitive impairment by inhibiting renewal and replacement of oligodendrocytes in adults or development of oligodendrocytes in children. Further, our results suggest an ISR inhibitor might attenuate the negative effect of EVG on the maturation of oligodendrocytes. Our findings also suggest that development of less toxic ART compounds and adjunctive therapies are needed to minimize the side effects of ART on the CNS.

LIST OF TABLES

LIST OF FIGURES

LIST OF ABBREVIATION

ART	Antiretroviral therapy
ASPA	Aspartoacylase
ANI	Asymptomatic Neurocognitive Impairment
ACC	Acetyl-CoA carboxylase
BBB	Blood Brain Barrier
BHLH-zip	Basic helix-loop-helix zipper
cART	Combined antiretroviral therapy
CCR5	CC-chemokine receptor 5
CXCR4	CXC-chemokine receptor 4
CSF	Cerebral Spinal Fluid
COBI	Cobicistat
CPE	CNS Penetration Effectiveness
DMSO	Dimethyl sulfoxide
DAPI	4′,6-diamidino-2-phenylindole
EVG	Elvitegravir
ER	Endoplasmic Reticulum
eIF2α	Eukaryotic translation initiation factor 2 (eIF2α) protein
ETC	Emtricitabine
FASN	Fatty acid synthase
GFAB	Glial fibrillary acidic protein
GCN2	General control nonderepressible 2
GalC	Galactocerebroside
GRP78	78 kD Glucose Regulated Protein

gp120	Glycoprotein 120
HIV	Human Immunodeficiency Virus
HMGCR	3-Hydroxy-3-Methylglutaryl-CoA Reductase
HAD	HIV-Associated Dementia
HAND	HIV Associated Neurocognitive Disorder
INSTIs	Integrase Strand Transfer Inhibitors
IBA1	ionized calcium-binding adapter molecule 1
ISR	Integrated Stress Response
Insigs	insulin-induced gene
LFB	Luxol Fast Blue
MBP	Myelin Basic Protein
MND	Mild Neurocognitive Disorder
NRTIs	Nucleoside reverse transcriptase inhibitors
NNRTIs	Non-nucleoside reverse transcriptase inhibitors
NMDAR	N-methyl-D-aspartate receptor
NPCs	Neuronal Progenitor Cells
OPCs	Oligodendrocytes Precursor Cells
PIs	Protease Inhibitors
PERK	PKR-like ER kinase
PKR	Double-stranded RNA-dependent protein kinase
PP1	Protein Phosphatase 1
PPP1R15A	Protein Phosphatase 1 Regulatory Subunit 15A
PPP1R15B	Protein Phosphatase 1 Regulatory Subunit 15B
PLP	Proteolipid Protein

PNS	Peripheral Nervous System
RAL	Raltegravir
RIT	Ritonavir
Scap	SREBP Cleavage Activating Protein
S1P	Site-1 protease
SREBP	Sterol regulatory element-binding protein
TUNEL assays	Terminal deoxynucleotidyl transferase dUTP nick end labeling
TAF	Tenofovir Alafenamide
TDF	Tenofovir Disoproxil Fumarate
TRANS-ISRIB	Integrated Stress Response Inhibitors
UPR	Unfolded Protein Response
WHO	World Health Organization
XBP-1	Xbox Binding Protein-1

CHAPTER 1: Introduction

1.1 <u>Overview</u>:

Since the isolation of Human Immunodeficiency virus (HIV) three decades ago, research has revealed many aspects of this virus including the interaction with host cells and other pathogenic mechanisms. HIV is a lentivirus within the family of retroviridae, it's a single strand RNA virus which has two types, HIV-1 and HIV-2 [1]. Like other retroviruses HIV-1 virions contain two copies of a single-stranded RNA genome, which is reversely transcribed to double-stranded DNA by the viral reverse transcriptase enzyme. This double-stranded DNA fragment is subsequently integrated into the host genome by the viral integrase enzyme [2]. Although HIV-induced abnormalities do not manifest in the CNS until the later stages of infection, there is evidence to support early entry of virus into the CNS in HIV-1 positive patients [3]. However, the major impact of HIV on neuronal cells likely occurs indirectly through release of excitotoxic substances from HIV infected macrophages [4-7]. A major manifestation of HIV in the CNS is HIV associated neurocognitive disorder (HAND) [8]. The development of combined antiretroviral therapy (cART) transformed the HIV infection from a lethal disease into a chronic illness managed by medication [9]. cART is a combination of antiretroviral compounds that target different points in the viral life cycle and fall into several categories:

1. Nucleoside reverse transcriptase inhibitors (NRTIs)
2. Non-nucleoside reverse transcriptase inhibitors (NNRTIs)
3. Protease inhibitors (PIs)
4. Integrase inhibitors (INSTIs)

5. Fusion inhibitors (FIs)

6. Chemokine receptor antagonists (CCR5 antagonists)

It has been found that using multiple classes of ART is more effective at viral suppression compared with treatment using a single class [10]. Despite viral suppression with cART, about 50% of HIV-positive patients still suffer from HAND. Previously, our lab showed that using ritonavir (RIT) (a protease inhibitor) had a negative effect on the differentiation of oligodendrocytes suggesting that RIT contributed to the loss of white matter in HAND [11]. One of the prominent cellular stress responses associated with ART treatment is ER stress, generated from the accumulation of unfolded proteins inside the lumen of ER, which is a candidate for the major underlying mechanism for much of the damage observed in the CNS of patients with HAND receiving ART in their treatment for HIV [12]. Another potential factor that contributes to the neurological damage in HAND is through disturbance of lipid balance in the oligodendrocytes in patients using RIT as part of their cART regimen [13]. We hypothesized that different classes of cART compounds activate different cellular stress pathways in oligodendrocytes. Attenuating these stresses could have a therapeutic impact and could ameliorate negative effects of cART drugs on oligodendrocytes.

1.2 HIV-Associated Neurocognitive Disorder (HAND)

According to the latest statistics from the world health organization (WHO), thirty-seven million people are infected with human immunodeficiency virus-1 (HIV-1) worldwide[14]. Approximately half of all HIV-positive patients clinically present with a neurological manifestation called HIV-associated

neurocognitive disorder (HAND), a spectrum of cognitive, motor, and behavioral abnormalities associated with white matter loss [8]. HIV enters the brain within the first two weeks of infection [15]. Several mechanisms have been proposed in the literature to explain how HIV infects the CNS. One theory holds that the virus can infect the endothelial layer of the blood brain barrier (BBB) and damaging the endothelial layer by the virus results in easier access of the virus to the CNS [16]. Another theory suggests that the HIV disrupts the lipid rafts in the cell membrane of the endothelial layer of BBB which is an important portal into the CNS [17]. Lastly, the most widely accepted theory is the "Trojan horse" theory, through which HIV-1 infected monocytes pass through the BBB leading to subsequent viral release and propagation in the CNS with the pool of infected macrophages spreading HIV infection inside the brain [18]. In the CNS, the virus can infect macrophages, microglia, and a small proportion of astrocytes. However, HIV-1 has not been known to elicit any direct effects on neurons or oligodendrocytes [19-21]. Two proposed mechanisms explain the effects of the HIV on the neuronal cells, the first proposed mechanism is through direct injury from HIV proteins (e.g. gp120, Tat, and Vpr) released from infected macrophages and microglia which interact with receptors on neurons. The second proposed mechanism is the "bystander effect" hypothesis, which suggests that the damage occurs due to the release of cytotoxic molecules including reactive oxygen species, nitric oxide, glutamate, and pro-inflammatory cytokines and chemokines from the infected immune cells in the CNS, leading to neuronal damage and dysfunction [7]. Both direct viral protein effects and indirect bystander effects of HIV have been documented in the literature and result in HIV-mediated

neuronal toxicity in HAND patients [22]. HAND severity is clinically divided into three categories based on two specific factors: patient neurocognitive status and patient functional status. Based off of these two criteria, patients can be diagnosed as having Asymptomatic Neurocognitive Impairment (ANI), Mild Neurocognitive Disorder (MND), or HIV Associated Dementia (HAD). HAD is considered the most severe form of HAND (Table1) [8].

	Neurocognitive Status	Functional Status
Asymptomatic Neurocognitive Impairment (ANI)	1 SD below mean, 2 cognitive domains	No impairment in activities of daily living
Mild Neurocognitive Disorder (MND)	1 SD below mean, 2 cognitive domains	Impairment in activities of daily living
HIV Associated Dementia (HAD)	2 SD below mean, 2 cognitive domains	Marked impairment in activities of daily living

Table 1: Categories of HIV associated neurocognitive disorder HAND. Neurocognitive status included test of at least five domains such as language, attention-formation processing and simple motor skills. The functional status is usually evaluated by self-report.

HAD incidence significantly decreased during the post-cART era [8, 23]. Currently, $CD4^+$ T-lymphocyte cell counts are no longer a marker for HAND severity. Instead, cerebrospinal fluid (CSF) analysis and neuroimaging techniques can be utilized to detect pathological changes in the CNS. This has proven especially useful for patients with accelerated progression of dementia. Before the cART era, approximately 25% of HAND positive patients had the severe form of HAND (HAD) with neuronal death observed in the

frontal lobes, hippocampus, and basal ganglia [24]. Since cART introduction in the mid 1990s, an extensive clinical investigation has revealed a dramatic reduction in the prevalence of HAD (specifically, to only 2% of HIV-1 positive patients). However, the milder forms of HAND became more predominant, with a shift from pre-cART subcortical pathology to cortical manifestations with cART. It is also interesting to note that the percent of HIV-1 patients with HAND remains unchanged from the pre-ART to the post-ART eras [25-29]. CNS damage in the post-cART era has been attributed to multiple factors such as irreversible brain impairment prior to cART initiation, poor CNS penetrance of several ART drugs, and inadequate viral elimination from CNS. More importantly, ART drugs themselves have been shown to have deleterious effects on the CNS [7, 11, 12, 30, 31].

1.3 <u>Antiretroviral Therapy:</u>

Prior to 1990s, HIV-1 antiretroviral drugs were administered as a monotherapy, but due to the error-prone reverse transcription process during viral replication, HIV is highly susceptible to mutations. However, in the late 1990s, the standard of care changed such that several ART drugs could be administered with a lower pill burden to combat HIV-1, which became known as combined antiretroviral therapy (cART) to overcome the high mutation rate of HIV [32]. This multiple-hit approach targets the virus at several different biological processes to control viral replication, and to transform HIV-1 infection from a lethal illness into a chronic, yet manageable disorder [33-35]. It is important that after cART initiation, treatment should not be interrupted. ART cessation has been associated with opportunistic infections and further

immune system compromise [36]. ART has no therapeutic effect on previously infected cells, but it prevents further HIV-1 infection of new target cells with high efficacy [37]. ART drugs have been designed to simultaneously target the virus at one of the five stages of the HIV-1 life cycle, viral entry, reverse transcription, viral DNA integration into the host genome, transcription, virus assembly/production, and proteases [32, 38]. The multiple classes of ART suppress the virus in different ways (Figure 1); the entry inhibitor class interferes with viral entrance into the host cell. It works by inhibiting virus attachment to the CD4 receptor, and co-receptor CC-chemokine receptor 5 (CCR5) or CXC-chemokine receptor 4 (CXCR4) which is necessary for fusion of the virus to the target cell membrane [39]. The Nucleoside reverse transcriptase inhibitors (NRTIs) mimic endogenous deoxyribonucleotides and are characterized by having high affinity for the virus reverse transcriptase enzyme, which facilitates incorporation into the viral DNA strand during synthesis [40]. Non-nucleoside reverse transcriptase inhibitors (NNRTIs), unlike NRTIs, disrupt the enzymatic activity of the viral reverse transcriptase [41]. Integrase strand transfer inhibitors (INSTIs) are one of the more recently-developed classes of antiretrovirals. These drugs inhibit the HIV-1 integrase enzyme, which is important for viral DNA integration into the cell genome. Specific drugs in this class include Elvitegravir (EVG) and Raltegravir (RAL). Integrase inhibitors bind to cofactors of the viral integrase enzyme that are important for interaction with the host DNA resulting in blocking the insertion of the virus into the host genome [42]. The protease inhibitor (PI) class has a high affinity for the HIV protease active

site. Inhibiting this enzyme prevents HIV maturation and subsequent viral budding (Figure 1) [43].
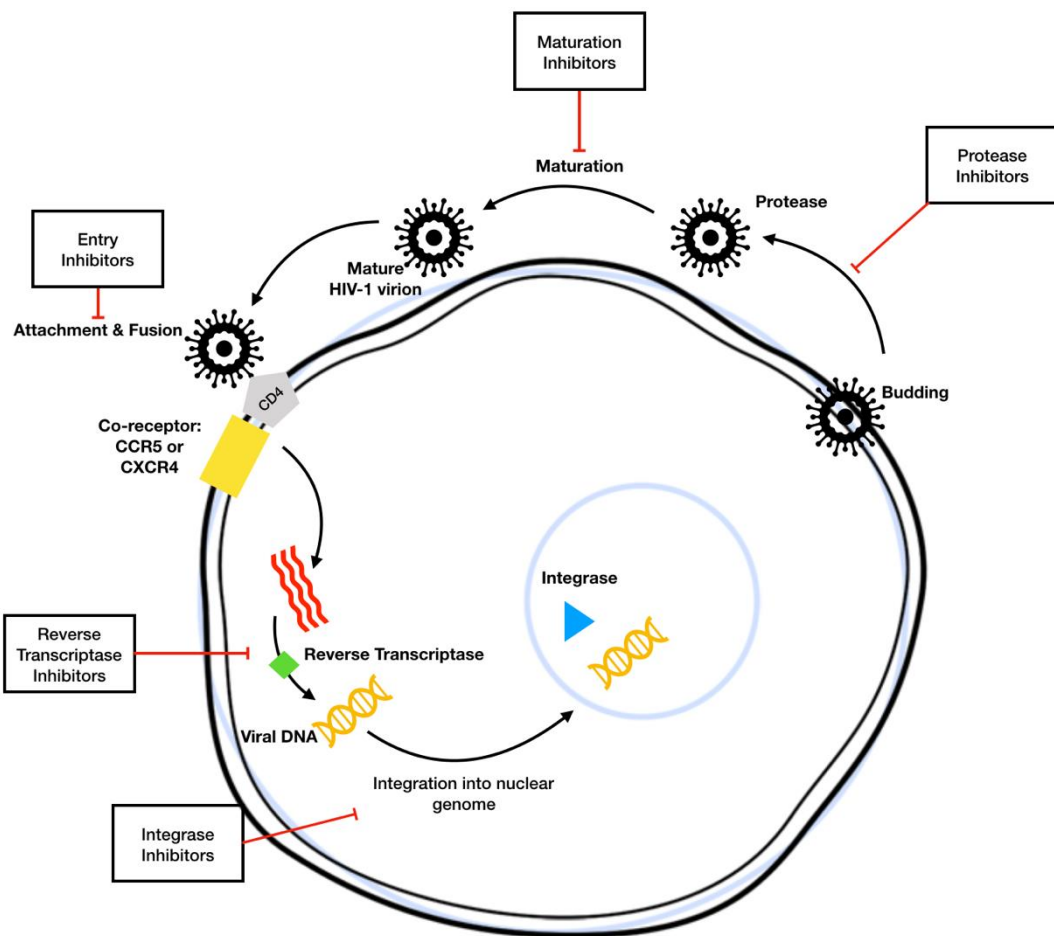
Figure 1: Classes of ART; Treatment of HIV infected patients is usually a combination of these classes that aim at suppressing the life cycle of the virus at different points.

These drugs are usually prescribed with pharmacokinetic boosters, such as the P450 inhibitors Cobicistat (COBI) or RIT [44]. Both COBI and RIT are potent inhibitors of the cytochrome P450 isoenzyme and achieve the desired goal of boosting plasma drug concentrations, but COBI is more selective than RIT to P450 [45, 46]. A proposed cause for the persistence of the viral effects in the CNS is limited penetration of ART into CNS because of the presence of BBB. For this reason, a proposed method to eliminate viral reservoirs is to apply therapies with ART that would reach therapeutic concentrations in the

CNS tissue of infected patients [47]. To address the issue of ART penetration into the CNS, a CNS penetration effectiveness (CPE) score was developed based on 1) Chemical properties of the drug, 2) Concentration of the drug in CSF, and 3) Effectiveness of the drug to reduce the viral load in CSF [48]. One of the examples for that is EVG, a small lipophilic molecule that has been characterized to have a high CPE score [9, 49]. Still CPE scores do not completely correlate with CNS neurological functions, since several ART drugs with high CPE were associated with worse neurocognitive performance [50]. Our knowledge of the effects of CPE scores on neurological outcomes in human patients is limited due to technical and ethical limitations. Moreover, other factors are not included when evaluating the CPE such as drug and alcohol abuse, co-infections, and, most importantly, the integrity of BBB [51, 52]. Toxic effects of ART in the CNS have not been studied thoroughly, however with the periphery as an indicator it is likely that ARV drugs have the capacity to contribute to neuronal damage and manifestations of HAND.

1.4 <u>The Integrated Stress Response (ISR)</u>

One of the protective cellular mechanisms in response to different stressors is the activation of a common adaptive pathway termed the integrated stress response (ISR). Extracellular and intracellular stressors such as hypoxia, amino acid deprivation, glucose deprivation, viral infection, or the accumulation of unfolded proteins in the ER can activate this pathway [53]. The pathway is initiated by one of four protein sensors in unstressed cells. These four proteins are PKR-like ER kinase (PERK), double-stranded RNA-dependent protein kinase (PKR), heme-regulated eIF2α kinase (HRI), and

general control nonderepressible 2 (GCN2) (Figure 2) [53, 54]. The common point where these kinases converge to activate ISR is the phosphorylation of eukaryotic translation initiation factor 2 subunit alpha (eIF2α) on serine 51 [55]. Each of these kinases are activated by different stressors. PERK can be activated by accumulation of unfolded proteins in the lumen of ER, perturbations in calcium homeostasis, or changes in cellular energy or redox status [56]. There are two models of activation of PERK through ER stress. The classical model is through the accumulation of incompletely folded or unfolded proteins in the lumen of ER leading to dissociation of GRP78 from PERK leading to activation and autophosphorylation [57, 58]. However, another model suggests that PERK is activated directly by binding of unfolded proteins to its luminal domain [56]. GCN2 becomes activated in response to amino acid deprivation [59]. PKR is activated mainly by double strand RNA viruses [60, 61]. Unlike other kinases, stressors like ER stress, oxidative stress, growth factor deprivation and bacterial infection can also activate PKR kinase in a dsRNA-independent manner [62]. HRI is activated upon heme deprivation leading to dimerization and autophosphorylation of its kinase domain [63]. In the ISR, restoring normal cellular function is performed by dephosphorylating eIF2α, which is accomplished by protein phosphatase 1 (PP1), PPP1R15A (known as GADD34), or PPP1R15B (known as CReP). CReP operates under resting-state conditions to maintain a low level of eIF2α phosphorylation, unlike GADD34. GADD34 expression is induced at later stages of the ISR, acting as part of an important negative feedback loop to restore normal protein synthesis once the stress has been resolved (Figure 2) [64, 65].
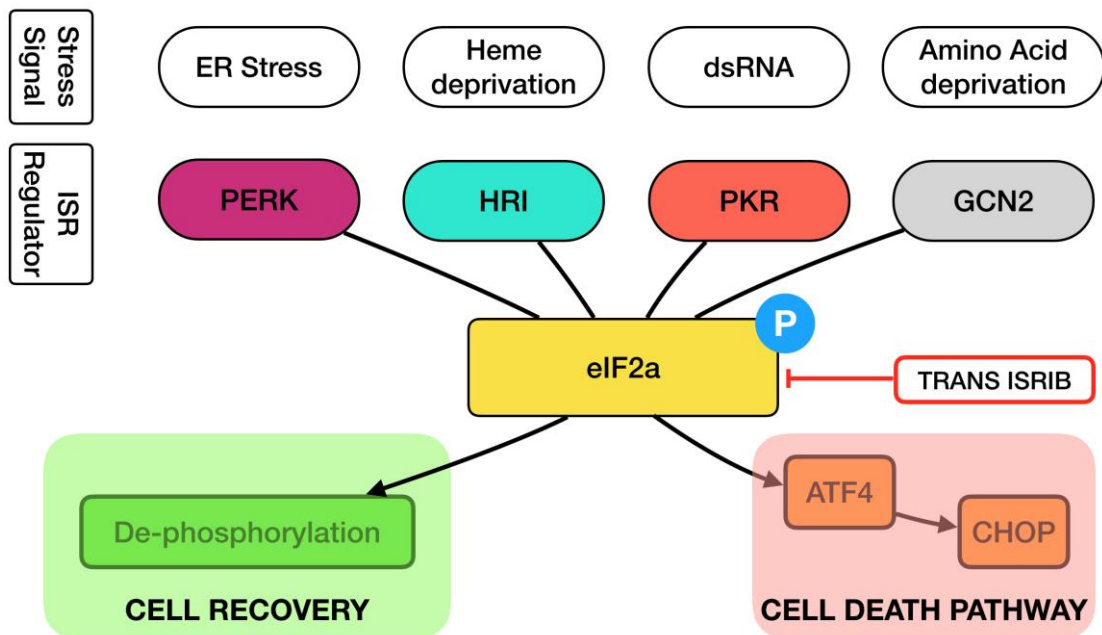
Figure 2: Integrated Stress Response (ISR): ISR is a common pathway activated for adaptation to various intrinsic and extrinsic stressors. These stressors activate one of four kinases which are PKR-like ER kinase (PERK), double-stranded RNA-dependent protein kinase (PKR), heme-regulated eIF2α kinase (HRI), and general control nonderepressible 2 (GCN2). The common point where these kinases converge to activate ISR is the phosphorylation of eukaryotic translation initiation factor 2 (eIF2α). Cellular normal function will be restored upon dephosphorylating eIF2α and in case of persistence of the stress, ATF4 will mediate cell death through activation of CHOP.

1.4a ISR Activation by ART Drugs

ART has improved the quality of life of HIV-positive patients and transformed HIV from a mortal disease into a chronic disease. However, a large number of studies show that ART contributes to other conditions such as HAND, dyslipidemia and other disorders [11, 66, 67]. A few previously published studies show that different classes of ART are responsible for activation of different stress pathways in neural cells. RIT from the PI class inhibits the differentiation of oligodendrocytes through an as yet unidentified pathway[11] and lopinavir and EVG are toxic to neurons [12]. Another study performed on primary neurons showed that EVG treatment decreased the maturation and

elongation of neuronal processes and activated the ISR, as assessed by measuring the levels of phosphorylated eIF2α. Most notably, the effects from EVG treatment were significantly reduced after pharmacologically blocking eIF2α phosphorylation with a drug called TRANS-ISRIB.[12] However, the literature on the effects of HIV ART on the different stress pathways in the CNS is incomplete.

1.5 <u>White matter pathologies in HAND</u>

During HIV-1 infection/HAND, white matter changes compromised structural integrity and volume of corpus callosum, internal capsule, superior longitudinal fasciculus, superior corona radiata, as well as reduction in overall blood flow to white matter. Cognitive impairment was positively correlated with white matter injury, but not to the viral load [11, 68-73]. Furthermore, a recent transcriptome analysis identified genes which remain dysregulated in HAND-afflicted individuals on ART including important myelin genes such as myelin-associated oligodendrocyte basic protein, myelin transcription factor 1, and myelin basic protein [74]. One of the earlier treatment regimens for HIV (which is still part of the World Health Organization treatment guidelines) includes RIT and lopinavir [14]. Treatment with these protease inhibitors caused a reduction in the maturation and differentiation of OPCs *in vitro* and RIT treatment reduced myelin protein expression *in vivo* [11, 75]. The new guidelines for patients with HIV infection include a more recently-introduced class of drugs called integrase strand transfer inhibitors (INSTIs) which inhibit the integrase enzyme encoded by the virus to integrate its genome into the host cell DNA, which is an essential process for HIV replication [9, 44]. Here,

we test two different INSTIs: EVG and RAL, and their effects on OPC survival

and differentiation *in vitro* using primary rat cortical cell culture model, and the

effects of EVG combined with P450 inhibitor, cobicistat, to examine the effect

of the drug on the myelination of oligodendrocytes in a cuprizone mouse

model [76, 77].

1.6 <u>Sterol regulatory element-binding protein (SREBP) pathway</u>

The myelin in mammals is synthesized by two types of cells, oligodendrocytes

in the CNS and Schwann cells in the peripheral nervous system (PNS) and is

a lipid rich and multilamellar structure. Beside providing nutrition and support,

oligodendrocytes and Schwann cells play a major role in insulating the nerve

axon to improve electrical conductivity. Myelin plays a major role in higher

brain function and a reduction in the myelin production is associated with

diseases such as multiple sclerosis (MS) [78]. The plasma membrane of

oligodendrocytes differs from other cells due to the presence of a high lipid

content in its membrane [79]. During myelination, oligodendrocytes generate

tremendous amount of lipids in a short period of time [80]. Unlike other cells,

the protein to lipid ratio is 1 to 186 due to the compact function of the most

abundant proteins in myelin MBP and PLP [81]. Quantitively, the most

abundant lipids in myelin are cholesterol and fatty acids. The cholesterol

provides the stability to myelin through regulating permeability and fluidity of

the membrane, the rate of cholesterol synthesis appears to couple with the

speed of myelin membrane biogenesis [82]. Knocking out fatty acid synthesis

in mice is embryonically lethal, and resulted in reduced thickness of the

myelin wrapping of nerve axons [83, 84]. The intracellular levels of both

cholesterol and fatty acids are precisely controlled through a feedback system facilitated by a family of transcription factors called sterol regulatory element-binding proteins (SREBPs) which are members of the basic helix-loop-helix-leucine zipper (bHLH-Zip) transcription factor family. SREBPs are found as inactive precursors bound to the ER membrane. A reduction in cholesterol and fatty acids results in activation of SREBPs through their translocation from the ER membrane to the Golgi apparatus where they are cleaved by site 1 protease (S1P) and site 2 protease (S2P). S1P cleaves SREBPs in the luminal loop between the two membrane-spanning sequences, whereas S2P cleaves the NH_2-terminal bHLH-Zip domain of SREBPs, releasing the mature forms. The mature NH_2-terminal domain then translocates to the nucleus to activate genes controlling lipid synthesis. In contrast, excess of lipids will result in SREBP inactivation to inhibit the accumulation of the lipids in the cell [85]. Cholesterol synthesis is controlled by two intracellular sensors; Insig and Scap. In case of cholesterol depletion, Insig-1 dissociates from Scap and is degraded by proteasomes, whereas the Scap/SREBP complex exits the ER and is transported to the Golgi apparatus where it is cleaved by both S1P and S2P and the active domain transfers into the nucleus to restore the cholesterol levels in the cell [86]. After sufficient production of cholesterol Insig binds to Scap forming Insig/Scap complex in the ER [87]. In sterol and fatty acid depleted cells, Insig is ubiquitinated by gp78. Ubiquitin regulatory X domain-containing protein 8 (Ubxd8) recruits the ATPase p97 to Insig leading to degradation of Insig by proteasomes, whereas this action is inhibited by the presence of unsaturated fatty acids and sterols [88]. Excess lipids in the body is a risk factor for developing disorders such as atherosclerosis which is a life

27

threatening disease, which results from lipid accumulation in the subendothelial matrix [89, 90]. An increase in the synthesis of fatty acids in the tissue is also associated with improper brain development besides other tissue dysfunctions [91].

1.7 <u>Oligodendrocytes in HAND:</u>

Oligodendrocytes are one of the four glial cells in the CNS, accounting for 5-8% of all glial cells [92]. Oligodendrocytes develop prenatally and early in postnatal life, and during development. Neural progenitor cells (NPCs) give rise to neurons and glial cells. However, oligodendrocytes are derived from oligodendrocyte precursor cells (OPCs). The three main stages of oligodendrocyte differentiation are: oligodendrocyte precursor cells (OPCs), immature oligodendrocytes, and mature oligodendrocytes [93]. Oligodendrocytes are generated from OPCs and mature in a stage-specific process, allowing for assessment using stage specific antigens. As they differentiate, they start expressing markers such as A2B5, NG2 and PDGF-A. As they transition into the immature stage, they express GalC and start to extend their processes to adopt the morphology of the mature phase which is characterized by the presence of PLP and MBP proteins (Figure 3) [94]. Ultimately, these proteins will form the myelin sheath as part of the oligodendrocyte plasma membrane. OPC founder cells arise from the ventricular region early during development as a result of local signaling by factors including sonic hedgehog. The immature oligodendrocyte is suggested to be highly migratory, and the final matching between oligodendrocytes and nerve axons happens due to combination of local regulation of cell

proliferation and differentiation [95]. The wrapping of multiple nerve axons by a solitary oligodendrocyte is a heavily synchronized event. Oligodendrocytes do not wrap different nerve axons at different time points. Rather, it is done within a short period of time, typically within 12 to 18 hours [96]. In the CNS, a single oligodendrocyte can produce as many as forty segments on multiple axons. The main elements of myelin in the oligodendrocytes are lipids, which account for at least 70% of dry weight, which is considered to be twice as concentrated as other plasma membranes.

Myelin's main function is to insulate the nerve axons to increase the electrical resistance in the cell membrane and decrease membrane capacitance to ensure fast conduction of electrical impulses [97, 98]. The myelin sheath also supplies nutrition and support for nerve axons[95]. Re-myelination or myelin repair of the nerve axons enables restoration of saltatory conduction, and a return of normal function lost during demyelination [92, 99]. Remyelination of the nerve axons after injury is not performed by mature oligodendrocytes, but rather by the OPCs distributed throughout the CNS.

Oligodendrocytes are thought to be not directly infected by HIV. Similar to neurons, oligodendrocytes lack the CD4 receptor required for HIV entry, suggesting that in these two populations indirect injury results from infected cells in the CNS [100]. The synaptodendritc injury in HAND is largely mediated by infected and activated microglia and astrocytes. In culture, HIV-1 Tat caused death of immature oligodendrocytes, while more mature OLs remained alive with dysregulated myelin protein and morphology [101]. In humans, the transcriptome analysis showed an alteration in oligodendrocyte

specific genes following HIV-infection in HAND patients, this alteration remained even after suppression of the virus with ART [74]. Our studies demonstrate that selected ART drugs inhibit oligodendrocyte precursor cell differentiation, suggesting that it might contribute to the development of HAND. *In vitro* we were able to rescue the differentiation of oligodendrocytes from the effects of one ART drug. Our findings also suggest that development of less toxic ART compounds and adjunctive therapies are needed to minimize the side effects of ART in the CNS.
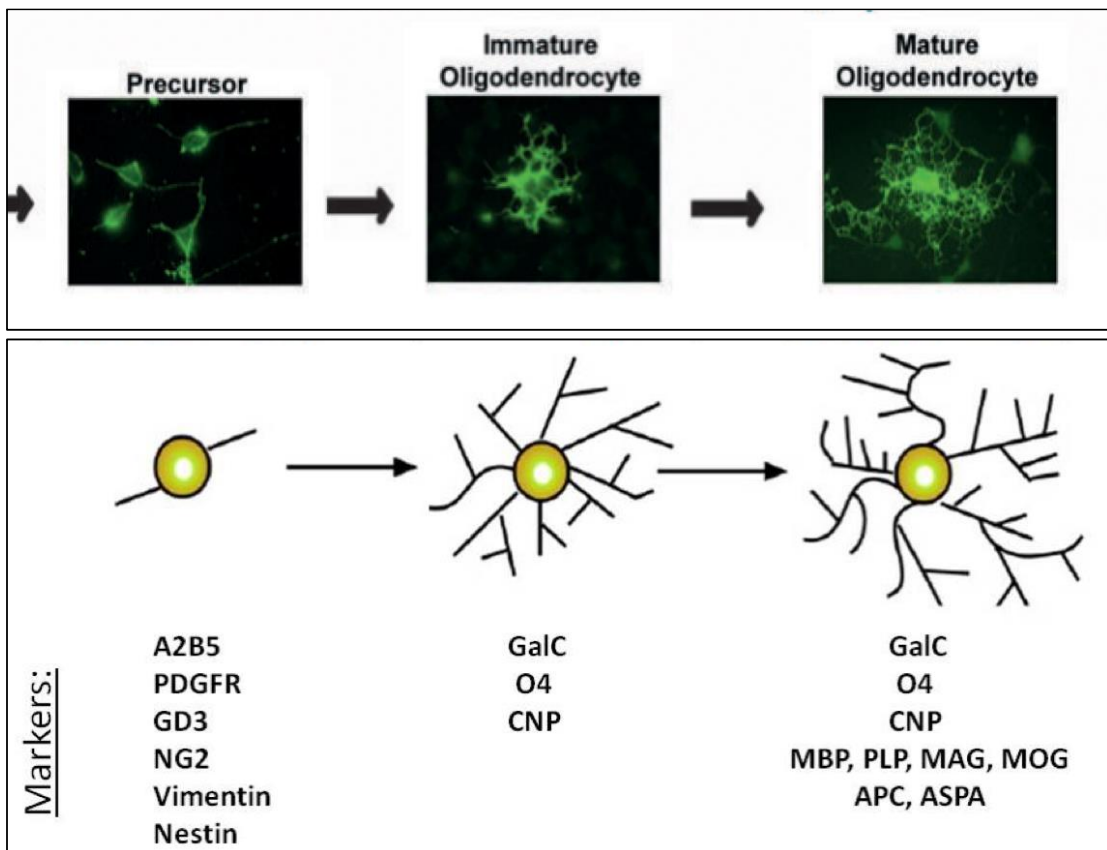
Figure 3: Progression of oligodendrocyte lineage from OPCs to mature cells; specific markers found at different stages of maturation of oligodendrocytes during their development. Monitoring these markers, using specific antibodies, allows for studies to be performed evaluating maturation from oligodendrocyte precursor cells to immature and mature oligodendrocytes.

CHAPTER 2: The role of specific *Integrase Strand Transfer Inhibitors* (INSTIs) in modulating oligodendrocyte maturation and myelination in HAND

2.1 <u>Abstract</u>

Despite effective viral suppression through combined antiretroviral (ARV) therapies (cART), approximately half of HIV-positive individuals present with HIV-associated neurocognitive disorder (HAND), a spectrum of cognitive, motor, and behavioral disturbances. Clinical manifestations of HAND include non-specific gliosis, synaptodendritic damage, and myelin loss. Studies of cART-treated patient brains have shown persistent myelin abnormalities including the thinning of the corpus callosum, and decreased myelin protein mRNAs. The myelin membrane, produced by oligodendrocytes, is critical for rapid action potentials and axonal maintenance; thus, myelin loss can contribute to neurocognitive dysfunction. We have previously shown that ART compounds from the protease inhibitor (PI) class, ritonavir, attenuated maturation of oligodendrocytes, *in vitro* and *in vivo*. Current guidelines for cART regimens recommend a new class of ART compounds, the integrase strand transfer inhibitors (INSTIs). We hypothesized that INSTIs also alter maturation and/or survival of oligodendrocytes, contributing to the myelin loss seen in HAND patients. To address this question, we induced differentiation of primary rat oligodendrocyte progenitor cells in the presence or absence of therapeutically relevant concentrations of INSTIs elvitegravir and raltegravir. We found that INSTI raltegravir had no effect, while elvitegravir treatment resulted in a dose-dependent reduction in mature oligodendrocytes after three days. *In vivo* daily administration of elvitegravir to adult mice in the three

weeks following cuprizone-induced demyelination, resulted in reduced remyelination compared with cuprizone treated animals permitted to recover or treated with the vehicle. Elvitegravir treatment resulted in activation of the integrated stress response (ISR) in both our *in vitro* model of oligodendrocyte development and our *in vivo* model of remyelination. Blocking ISR with the inhibitor, Trans-ISRIB, rescued oligodendrocyte maturation in the presence of elvitegravir *in vitro*. These studies suggest that elvitegravir inhibits the maturation of oligodendrocyte precursor cells and subsequent myelination by oligodendrocytes.

Significance Statement

HIV-associated neurocognitive disorder (HAND) represents a spectrum of cognitive, motor, and behavioral disturbances that occur in approximately 50% of HIV-positive individuals, regardless of the consistent administration of combined antiretroviral (ARV) therapies (cART). The etiology and pathogenesis of HAND are currently unknown; however, soluble factors from HIV-infected macrophages/microglia and potentially cART themselves may play a role. Herein, we show that maturing oligodendrocytes treated with a front line ART compound, elvitegravir, are inhibited from differentiating into immature and mature oligodendrocytes. *In vivo* administration of elvitegravir to mice recovering from cuprizone-induced demyelination leads to attenuation of remyelination. We also show that elvitegravir treatment induces the integrated stress response (ISR) in oligodendrocytes *in vitro* and *in vivo*. Further, pretreatment with an ISR inhibitor, trans-ISRIB, prior to elvitegravir treatment, rescued maturation attenuation induced by elvitegravir *in vitro*.

32

2.2 <u>Introduction</u>

Despite effective viral suppression by combined antiretroviral (ARV) therapy (cART), approximately 50% of HIV-positive patients present with a broad spectrum of cognitive, motor, and behavioral disturbances collectively termed HIV-associated neurocognitive disorder (HAND) [8, 102-104]. Due to the high mutation rate during HIV replication, cART is designed to target multiple processes in the replication cycle of the virus to reduce drug resistance [105]. The newest class of ART compounds, the integrase strand transfer inhibitors (INSTIs), inhibits the function of the virally-encoded HIV integrase enzyme which mediates integration of the reverse transcribed viral DNA into the host cell genome [44, 105]. Current front-line cART regimes include two compounds from the nucleoside reverse transcriptase (NRTI) class and one from the INSTI class, making these compounds clinically relevant to study [14]. In the post cART era, HAND neuropathogenesis includes persistent microgliosis, astrogliosis, dendritic damage, neuronal, loss, synaptic loss and white matter abnormalities [8, 106, 107]. White matter changes include dramatic thinning of the corpus callosum and loss of structural integrity and volume of frontal white matter [68, 70, 72, 108]. Notably, the severity of cognitive impairment correlates with the amount of white matter damage [109]. Furthermore, a recent transcriptome analysis identified myelin-associated oligodendrocyte basic protein, myelin transcription factor 1, and myelin basic protein (MBP) as being reduced in patients with HAND regardless of cART [110]. In the CNS, oligodendrocytes are non-neuronal cells that produce white matter or myelin; this mostly lipid-based membrane is

critical for the rapid transmission of action potentials, metabolic support, and prevention of axonal degeneration [111-113].

Even with growing evidence of persistent myelin abnormalities in HAND individuals, the mechanism underlying these observed changes remains unclear [102, 107, 114]. cART suppresses viral replication to undetectable levels in the periphery; however, inflammation and viral reservoirs persist in the CNS [106, 115-117]. Additionally, ART compounds themselves may contribute to the pathogenesis of HAND [107]. ART-induced toxicity has been shown in primary rat cortical neurons [12, 31, 118].The integrated stress response (ISR) was identified as a mediator of ART-induced neurotoxicity by a subset of these compounds. Further, ISR activation has been observed in neurons and astrocytes of HAND patients [12, 31, 118]. The ISR is cytoprotective and activated in response to extrinsic and intrinsic stressors such as viral infections, and accumulation of unfolded proteins in the endoplasmic reticulum (ER), respectively; however, if the stress is left unsolved this ultimately leads to cell death [53, 119, 120]. Furthermore, our group has previously reported that ART compounds ritonavir and lopinavir, inhibit oligodendrocyte maturation, *in vitro*; ritonavir also inhibited myelin protein production, *in vivo* [11]. We hypothesized that new frontline ART compounds from the INSTI class, elvitegravir (EVG) and raltegravir (RAL), will also affect oligodendrocyte maturation and/or survival, contributing to the myelin abnormalities observed in HAND patients. Here, we examine INSTIs, EVG and RAL, on primary rat oligodendrocyte precursor cell (OPC) maturation and survival using a well-established *in vitro* model [94, 119]. Moreover, we test the effect of EVG on remyelination following cuprizone-

induced [77, 121, 122]. Finally, we show that the ISR mediates the effects of EVG in our *in vitro* oligodendrocyte maturation model. Our results support a role for INSTI, EVG, in myelin abnormalities seen in HAND patients and provides the first evidence to suggest the ISR as a mediating pathway that could be therapeutically relevant to these patients.

2.3 <u>Materials and Methods</u>

Chemicals and Reagents. The following antibodies used in this study were purchased from the indicated vendors: GeneTex (Irvine, CA): Aspartoacylase (ASPA; Cat# RRID:); Wako (Osaka, Japan): ionized calcium binding adaptor molecule 1 (IBA1; Cat# RRID:); Invitrogen (Carlsbad, CA): phospho-eukaryotic initiation factor 2 alpha (p-eIF2α; Cat# 44-728G RRID: AB_1500038); Cell Signaling Technology (Beverly, MA): eukaryotic initiation factor 2 alpha (eIF2α; Cat# RRID:), phospho-eukaryotic initiation factor 2 alpha (p-eIF2α; Cat# RRID:); BD Biosciences (San Jose, CA): platelet derived growth factor receptor alpha (PDGFRα, Ca# 556002 RRID: AB_396286); Sigma Aldrich (St. Louis, MO): alpha-tubulin (α-tubulin; Cat# T5168 RRID: AB_477579); Millipore (Temecula, CA): glyceraldehyde 3-phosphate dehydrogenase (GAPDH; Cat# MAB374 RRID: AB_2107445), neural/glia antigen 2 (NG2, Ca# AB5320 RRID: AB_11213678); BioLegend (San Diego, CA): myelin basic protein (MBP; Cat# 808401 RRID: AB_2564741); Proteintech (Rosemont, IL): activating transcription factor 4 (ATF4; Cat# 10835-1-AP RRID: AB_2058600), lamin B1 (Ca# 12987-1-AP RRID: AB_213690). Additional antibodies were: galactocerebroside (GalC) mouse hybridoma supernatant (GalC H8H9) (Ranscht et al., 1982), myelin basic

protein (MBP, rat hybridoma supernatant) and glial fibrillary acidic protein (GFAP) (kind gifts of Dr. Virginia Lee, University of Pennsylvania, Philadelphia, PA). The following chemical reagents used in the study were purchase from the indicated vendors: Sigma Aldrich (St. Louis, MO): poly-D-lysine (PDL), biotin, dimethyl sulfoxide (DMSO), Triton X-100, Fast Green FCF, insulin, protease inhibitor cocktail, thyroxine (T4), lithium carbonate, luxol fast blue, cuprizone, bovine serum albumin (BSA); Alfa Aesar (Lancashire, United Kingdom): cresyl violet; Jackson Immunoresearch Laboratories (West Grove, PA): FITC-conjugated goat anti-mouse IgG3, rhodamine-conjugated goat anti-rat IgG; LiCOR (Lincoln, NE): Odyssey goat anti-mouse IRdye 800CW, goat anti-mouse IRdye 680RD, goat anti-rat IRdye 800CW, goat anti-rat IRdye 680RD, goat anti- rabbit IRdye 800CW, goat anti-rabbit IRdye 680RD; Toronto Chemicals (Toronto, Canada): elvitegravir; ASTA Tech (Bristol, MD): cobicistat; Invitrogen (Carlsbad, CA): 4%– 12% Bis-Tris gradient gels, deoxyribonuclease 1 (DNase). R&D Systems (Minneapolis, MN): basic fibroblast growth factor (bFGF), platelet-derived growth factor-AA (PDGF-AA); PeproTech Inc. (Rocky Hill, NJ): neurotrophin-3 (NT3); Thermo Fisher Scientific (Waltham, MA): trypsin, B27 supplement, penicillin/streptomycin, Hank's balanced salt solution (HBSS), neurobasal medium, Dulbecco's modified Eagle's medium and Ham's F12 (DMEM/F12); Roche Diagnostics (Basel, Switzerland): biotin-16- dUTP; Vector Laboratories (Burlingame, CA): vectashield with 4',6-diamidino-2-phenylindole (DAPI); Biorad (Hercules, CA): precision plus protein kaleidoscope, tween-20, nitrocellulose membrane; Denville Scientific Inc. (Saint-Laurent, QC): HyBlot CL autoradiography film; Millipore (Temecula, CA): polyvinylidene fluoride

(PVDF) membrane. Tocris Bioscience (Bristol, UK): trans-ISRIB. Lonza (Walkersville, MD): L-glutamine.

Preparation of primary rat oligodendrocyte precursor cell cultures. All experiments were performed in accordance with the guidelines set forth by The Children's Hospital of Philadelphia and The University of Pennsylvania Institutional Animal Care and Use Committees. Primary rat oligodendrocytes precursor cells (OPCs) were isolated from brains of postnatal day 1 Sprague Dawley rats (Charles River Laboratories, Wilmington, MA RRID: RGD_737891) and plated on T75 flasks [11]. We purified the OPCs using the "shake-off" method [123]. Briefly, once OPCs reached confluency on T75 flasks, they were rotated on an orbital shaker set to 250 rpm and incubated overnight at 37°C. The following day, cells were filtered using a 20-µM nylon net (Merck Millipore, Darmstadt, Germany), followed by centrifugation at 1500 rpm for 5 min at 4°C. The supernatant was discarded, and the pellet was resuspended in neurobasal medium (5 mL), then incubated in a bacteriological petri dish for 15 min at 37°C and 5% CO_2. The supernatant is collected and centrifuged at 1500 rpm for 5 min at 4°C. The pellet was resuspended in growth media consisting of neurobasal media with B27 and growth factors: PDGF (2 ng/mL), NT3 (1 ng/mL) and FGF (10 ng/mL) and plated on 24-well plates with coverslips or 10 cm petri dishes.

Drug Treatments. Primary rats OPCs were grown in 24-well plates with coverslips or 10 cm petri dishes, for immunocytochemistry and immunoblot, respectively, until they reached about 70% confluency. To differentiate the

cells into mature oligodendrocytes, growth medium was replaced with differentiation media consisting of 50% DMEM, 50% Ham's F12, Pen/Strep, 2 mM glutamine, 50 µg/mL transferrin, 5 µg/mL putrescine, 3 ng/mL progesterone, 2.6 ng/mL selenium, 12.5 µg/mL insulin, 0.5 µg/mL T4, 0.3% glucose, and 10 ng/mL biotin. Simultaneously, the cells were treated with vehicle (DMSO), raltegravir (300 nM, 3.0 µM or 10 µM), elvitegravir (350 nM, 3.5 µM or 10 µM) or cobicistat (150 nM, 1.5 µM, 4 µM) for 72 hours, to allow differentiation to occur, before staining or protein collection [124]. Even though cobicistat is not active as an ARV, we examined the effect of cobicistat on oligodendrocyte maturation, *in vitro*, as it was used in our *in vivo* experiments to enhance administered elvitegravir concentrations. Pretreatments with Trans-ISRIB (5 µM) were 1 hour prior to elvitegravir (3.5 µM or 10 µM) treatment.

Immunofluorescence. Primary OPC cultures were prepared and stained as follows: coverslips were removed from wells and rinsed with PBS; then they were incubated with primary antibody for immature oligodendrocyte marker, GalC, diluted 1:4 in DMEM/12, for 30 min at room temperature. Coverslips were rinsed with PBS and incubated coverslips in FITC-conjugated goat anti-mouse secondary antibody, diluted at 1:200 in DMEM/F12, for 30 min at room temperature. Cells were fixed using 4% paraformaldehyde for 10 min then rinsed with PBS before incubation with a blocking/permeabilization solution containing 0.5% BSA and 0.1% Triton X-100 in PBS for 30 min. Cells were incubated in primary antibody for mature oligodendrocyte marker, MBP rat hybridoma supernatant, diluted 1:1 in PBS, for 30 min at room temperature.

Following a rinse with PBS, cells were incubated with rhodamine-conjugated goat anti-rat secondary antibody, diluted at 1:200 in PBS, for 30 min at room temperature. Cells were mounted on slides with vectashield mounting media containing DAPI (Vector Laboratories, Burlingame, CA). Cells were imaged using a Keyence BZ-X-700 digital fluorescent microscope (Keyence Corporation, Itasca, IL) affixed with UV, FITC, Cy3 and Cy5 filters. Images captured at 40x magnification were hand counted to quantify the number of immature and mature oligodendrocytes. Specifically, the number of immature and mature oligodendrocytes, identified as cells expressing GalC and MBP, respectively, was averaged across a total of 20 fields/coverslip with 2-4 coverslips/treatment condition for each biological replicate.

TUNEL Assay. To assess cells committed to apoptotic cell death, a TUNEL staining protocol, adapted from Gavrieli et al was used (Gavrieli et al., 1992). Cells were fixed with ice cold methanol for 10 min, washed with PBS, and permeabilized with 0.1% Triton X-100 and 0.5% BSA in PBS for 30 min. Positive control coverslips were generated during this time by incubating in DN buffer (30 mM Trizma base pH 7.2, 140 mM sodium cacodylate, 4 mM magnesium chloride, and 0.1 mM dithiothreitol) for 2 min, followed by DNase (1:200) in DN buffer for 10 min. All coverslips were washed with PBS, then placed in TDT buffer (30 mM Trizma base pH 7.2, 140 mM sodium cacodylate, 1 mM cobalt chloride) for 2 min. Cells were incubated for 1 hour at 37°C with TdT and biotin-UTP in TDT buffer (6 uL of each in 1 mL TDT buffer). After a subsequent PBS wash, cells were placed in TB buffer for 15 min (300 mM sodium chloride, 30 mM sodium citrate) and then a 2% BSA

solution for 30 min. Finally, cells were incubated with rhodamine-conjugated streptavidin for 20 min before a final PBS wash and mounting on slides with vectashield containing DAPI. Visualization and counting were performed as previously described [125].

RNA extraction and qPCR. The expression of MBP in oligodendrocyte cultures was quantified using quantitative reverse transcription polymerase chain reaction (RT-PCR). OPC cultures were grown on 100-mm dishes and harvested after 72-hour EVG treatment. RNA was extracted with Trizol, and RNA (5 µg) was converted to cDNA by the Invitrogen Superscript First-strand kit. Quantitative PCR was performed using Power SYBR Green, as previously described (Jensen et al., 2015). Samples were measured in triplicate for each experiment from 3 biological replicates (n = 3). Data were normalized using protein kinase gene 1 and analyzed according to the ΔΔCT method. Primer pairs obtained from Integrated DNA Technologies (Coralville, IA) for each gene are listed in Table 2.

MBP Forward for rat	5'- TGA AAA CCC AGT AGT CCA C-3'
MBP Reversed for rat	5'- GGA TTA AGA GAG GGT CGT C-3'
PLP Forward for rat	5'-TAG GAC ATC CCG ACA AGT-3'
PLP Reversed for rat	5'-AAA CAG GTG GAA GGT CAT T-3'

Table2: Primers used for qPCR for MBP and PLP gene

Immunoblotting. Whole cell extracts of primary rat oligodendrocyte cultures were prepared with cold cell lysis buffer (25 mM Tris (pH 7.4), 10 mM EDTA,

10% SDS, 1% Triton X-100, 150 mM NaCl containing protease and phosphatase inhibitor cocktails (PIs; Roche Diagnostics) followed by sonication and centrifugation at 10,000 rpm at 4°C for 30 min. Protein concentrations were determined by spectrophotometer ND-1000 from Thermo Fisher Scientific (Waltham, MA). Protein (7-20 µg) was loaded into each lane of 4% to 12% Bis-Tris gradient gels for separation. A broad-spectrum molecular weight ladder was run on each gel. After separation, proteins were transferred onto Immobilon-FL or nitrocellulose membranes and blocked in 5% milk for 30 minutes at room temperature. Membranes were incubated overnight at 4°C with primary antibodies in TBST + 5% BSA. Primary antibodies to the following antigens were used: MBP (SMI-99, 1:1000 dilution), α-tubulin (1:10000 dilution), ATF4 (1:1000 dilution), pEIF2α (1:1000 dilution, Cell Signaling), tEIF2α (1:1000 dilution), Lamin B1 (1:1000 dilution) and GAPDH (1:60,000 dilution). Following three washes in TBST, membranes were incubated with corresponding antigen specific fluorescent probe-conjugated secondary antibodies (1:10000 dilution) in TBST + 5% BSA. Membranes were visualized using an Odyssey Infrared Imaging System (LiCOR) or by film. Densitometric analysis of band intensities was conducted using the Odyssey Infrared Imaging System or by Fiji (NIH RRID: SCR_002285). All bands were normalized to the loading control, specified in each experiment.

Nuclear/Cytoplasmic Fractionation. For examination of activating transcription factor 4 (ATF4) nuclear cytoplasmic fractionation was performed. Briefly, 3-4 petri dishes of primary rat OPCs were stimulated to differentiate and treated

with vehicle (DMSO), EVG (3.5 µM) or positive control, thapsigargin (THAP, 500 nM). After 24 hours, cells were rinsed thoroughly with PBS and incubated at 4°C on a shaker (150 rpm) in the presence of cytoplasmic buffer (250 µL, 10 mmol/L HEPES, pH 7.9, 10 mmol/L KCL, 10 mmol/L EDTA, 1 mmol/L dithiothreitol, and 10% NP-40, supplemented with protease inhibitors) for 10 min. Extracts were centrifuged at 12600 rpm for 3 mins, and cytoplasmic supernatants were collected. The pellets were washed with cytoplasmic buffer (500 µL) and centrifuged again at 12600 rpm for 3 min. The pellets were then resuspended in nuclear buffer (100 µL, 20 mmol/L HEPES, pH 7.9, 400 mmol/L NaCl, 1 mmol/L EDTA, 1 mmol/L dithiothreitol, and 10% glycerol, supplemented with protease inhibitors) and incubated on an orbital shaker (200 rpm) at 4°C for 3 hours. Every 30 min the samples were vortexed at the highest setting for 10 sec. The nuclear supernatants were collected following centrifugation at 12600 rpm for 5 mins. All pellets were retained for potential analysis. Protein concentrations were determined the same as whole cell extracts (see above).

Cuprizone Model and In-vivo Drug Treatments. All experiments were performed following the guidelines set by Children's Hospital of Philadelphia Institutional Animal Care and Use Committee (IACUC) and University of Pennsylvania Institutional Animal Care and Use Committees. Six to eight week old C57BL/6 female mice were used for the cuprizone demyelination model (Jackson Laboratories, PA). Mice were divided into two groups: control and cuprizone-treated. Each group was then divided further into untreated, vehicle (DMSO)-treated, EVG/COBI-treated, with 10 female mice in the

untreated group and 5 per group in the rest. Control mice received normal powdered food for five weeks, while the cuprizone-treated mice received 0.25% cuprizone in their powdered food for five weeks. Both groups received normal food pellets during the last 3 weeks of the experiment. After 5 weeks of cuprizone feeding, 5 mice from each group, control and cuprizone were perfused, had brains removed and prepared for frozen section (see below) to determine to extent of the cuprizone lesion. At the same time point, other mice were implanted with IV cannula into the jugular vein and treated once daily with DMSO and/or EVG/COBI for the 3 week recovery period. For the implantation of the cannulas, sustained release buprenorphine (0.5-1.0 mg/kg) was administered at subcutaneous injection before the start of surgery. A ketamine/xylazine cocktail (80 and 12 mg/kg, respectively) was used to anesthetize the mice. A silastic IV cannula (CamCaths, Cambridge, UK) was inserted into the jugular vein, sutured in place using PERMA-HAND silk suture, (Ethicon Inc., Somerville, NJ) and mounted on the back of the mouse using a mesh back-mount. Over the course of the 3 week recovery period, mice were injected daily through the cannula with vehicle (DMSO) (5%), or EVG/COBI (65 mg/kg, diluted in DMSO).

Immunohistochemistry. Following the 5 weeks cuprizone or control feeding period and the extra 3 weeks DMSO or EVG/COBI injections, mice were terminally anaesthetized with a ketamine/xylazine cocktail and intracardially perfused with cold PBS and cold 4% paraformaldehyde (PFA, pH 7.4). Whole brains were isolated, post-fixed in 4% PFA for 2 hours and then cryoprotected with 30% sucrose in PBS for at least 24 hours. Serial coronal tissue sections

were cut at 12μm on a cryostat (Leica Microsystems, Exton, PA) throughout the entire corpus callosum, collecting three sections per slide[124, 126].

Mouse coronal tissue sections were stained as follows: we used ASPA (1:500 dilution) for labeling mature oligodendrocytes, NG2 (1:200 dilution) for labeling of OPCs, GFAP (1:1 dilution) for labeling astrocytes and IBA1 (1:500 dilution) for labeling microglia. All primary antibodies were diluted in GFAP in Feltri block (20% FBS, 80% PBS, 0.02% BSA, 0.001% Triton X-100, 0.02% NaN$_3$) and incubated overnight at 4°C. Following a PBS wash, slides were incubated for 30 mins at room temperature in rhodamine red-conjugated, goat anti-rabbit antibody (1:200 dilution, diluted in PBS) to visualize ASAP, FITC-conjugated, goat anti-rabbit antibody (1:200 dilution, diluted in feltri block) to visualize NG2, Cy5-conjugated, goat anti-rat antibody (1:200 dilution, diluted in PBS) to visualize GFAP, and FITC-conjugated, goat anti-rabbit antibody (1:200 dilution, diluted in feltri block) to visualize IBA1.

For pEIF2α staining, we used a tyramide amplification system (Perkin Elmer) following overnight incubation at 4°C with the primary antibody (1:3000 dilution, diluted in Feltri block, Invitrogen). Following a PBS wash, slides were incubated in biotin-conjugated, secondary antibody (1:600 dilution) for 30 mins at room temperature and then incubated in Fluorescein (DTAF)-conjugated Streptavidin (1:200 dilution, diluted in PBS) for 30 mins at room temperature (Jackson ImmunoResearch Laboratories). All slides were mounted in Vectashield with DAPI (Jackson ImmunoResearch Laboratories).

To count cells from frozen sections, brains from at least three mice were used per variable. Digital images were taken at 20 X magnification from sections at

the level of the anterior part of the corpus callosum, counting five 150 μm X 150 μm regions of interest per section, at least two sections per animal.

Luxol fast blue (LFB) staining. Mouse brain section slides were stained with 0.1% LFB, 0.1% Cresyl echt violet, and 0.05% lithium carbonate. The slices were dipped in 95% ethyl alcohol then incubated in LFB for 16-18 hours, followed by incubation in 95% alcohol for 2 minutes. The slides were then immersed in lithium carbonate solutions for another 2 minutes, followed by immersion in 70% ethyl alcohol for 30 sec. The slides were dipped quickly in water, and then incubated in Cresyl echt violt for 11 minutes at 56ºC. Finally, the slides were dipped in quick succession in 95% ethyl alcohol and xylene and then sealed with plastic covers using paramount.

Statistical analysis. For all rat cell culture experiments, primary OPC cultures prepared from each litter represents an independent biological replicate, and were treated with vehicle or drug in the indicated combinations. An untreated condition (UT) was also included within each biological replicate, and all results were normalized to this UT value. Repeated measures analysis of variance (ANOVA) was used to analyze these data to account for inherent correlations present within a single biological replicate. Data were analyzed using Graphpad Prism statistical software (version 7.0; RRID: SCR_002798) and were graphically presented as fold change or percent total from UT +/- standard error of the mean (SEM), with the UT condition represented by a dotted line.

2.4 Results

Elvitegravir reduces the number of immature and mature oligodendrocytes *in vitro*. Previously, our group has shown that ART compounds of the PI class, ritonavir and lopinavir, inhibit the maturation of oligodendrocytes, *in vitro [11]*. Using our well-established culture model [119], we examined whether INSTIs, elvitegravir (EVG) and raltegravir (RAL), inhibited oligodendrocyte maturation. EVG and RAL concentrations were based on reported plasma and cerebrospinal fluid (CSF) levels in humans, as measurements in human brain parenchyma have not been performed [127-129].

Clinically, EVG, is administered with cobicistat (COBI) because it is an inhibitor of cytochrome p450 enzymes in the liver, which metabolize EVG [44, 129]. Thus, by combining EVG with COBI, lower concentrations of EVG can be given to patients, to reduce side effects, while still achieving therapeutically relevant concentrations of EVG in the body. Even though COBI is not active as an ARV, we examined the effect of COBI on oligodendrocyte maturation as it is administered with EVG in patients. Briefly, OPCs were placed in differentiation media and treated with therapeutically relevant concentrations of EVG (350 nM, 3.5 µM, 10 µM), RAL (300 nM, 3 µM, 10 µM), or COBI (150 nM, 1.5 µM, 4 µM). After 72 hours, cultures were stained for transiently-expressed lineage specific proteins: GalC and MBP for immature and mature oligodendrocytes, respectively [130-133]. Representative images of drug-treated oligodendrocytes after 72 hours of differentiation showed dose-dependent decreases in differentiation in EVG-treated cultures compared with

vehicle-treated cultures, but not RAL- or COBI-treated cultures (Figure 4A). GalC-positive and MBP-positive cell counts demonstrated a dose-dependent decrease of differentiation into immature and mature oligodendrocytes, respectively, in EVG-treated cultures compared with vehicle-treated cultures, but not following RAL or COBI treatment (Figure 4B,C). This effect is mediated at the transcriptional level since our qPCR result showed a dose dependent reduction in MBP mRNA in cells treated with EVG (Figure.5)

Elvitegravir does not induce cell loss or apoptosis. In order to determine whether the decreased numbers of immature and mature oligodendrocytes observed following EVG treatment were due to inhibition of OPC maturation and not cell loss or apoptosis, we examined whether OPCs were dying by four measures, 1) numbers of DAPI-positive cell counts, 2) A2B5-positive cell numbers and 3) number of terminal UTP Nick end labeling (TUNEL) assay positive cells, which stains double-stranded DNA breaks, an early step in apoptotic cell death, and 4) number of cells staining for propidium iodide, a DNA intercalating agent that only passes through the membrane of necrotic cells, thus labeling nuclei of dying cells. After 72 hours of maturation, the number of DAPI- A2B5- positive cells did not change following EVG, RAL or COBI treatment (Figure 6A,B). Additionally, there was no increase in TUNEL-positive cells nor cells labeled with propidium iodide following EVG treatment (Figure 6C,D). DNase was used as a positive control for the TUNEL assay (Figure 6D). Together, these results suggest that EVG inhibits oligodendrocyte maturation in a dose-dependent fashion.

47

Elvitegravir treatment inhibits myelin protein production. Given that EVG-treated cultures contained fewer GalC- and MBP-positive cells, as compared with vehicle control, we next examined whether this effect resulted in decrease myelin protein levels. The cultures were treated as previously for 72 hours, protein was collected and processed for immunoblot analysis. The two doses of EVG (3.5 μM and 10 μM) resulted in a significant decrease in MBP levels when compared with vehicle (Figure 7A). In contrast, neither RAL nor COBI significantly altered MBP levels (Figure 7B,C). These data match that of the immunofluorescence results in Figure 4, with a large decrease in MBP-positive cells and MBP protein levels observed at 3.5 μM and 10 μM concentrations of EVG.

Elvitegravir-mediated inhibition of oligodendrocyte maturation is reversible. To determine if the effects of EVG were permanent, or if cells were capable of myelin protein production and localization once the drug was removed, we placed OPCs in differentiation media in the presence of 3.5 μM and 10 μM EVG and allowed 72 hours for maturation. At this time-point, a subset of cultures were washed and placed in drug-free differentiation media for an additional 24 hours. Cultures that underwent the drug washout period were stained for the same oligodendrocyte markers previously described and compared with cultures that did not undergo drug washout but were exposed to the same EVG treatments for 72 hours. As shown in Figure 4, 72 hour treatment with 3.5 μM EVG resulted in fewer GalC- and MBP-positive compared with vehicle; this effect was completely reversed after the removal of EVG (Figure 8B,C). Similarly, drug washout for 24 hours resulted in the reversal of reduced MBP expression levels following treatment with 3.5 μM

EVG as detected by immunoblotting (Figure 8D, E). In contrast, 24 hours after removal of the 10 μM concentration of EVG, the number of GalC- and MBP-positive cells remained reduced (Figure 8B,C). Similarly, drug washout for 24 hours did not rescue the reduction in MBP expression levels following 10 μM EVG treatment (Figure 8D,E).

Administration of elvitegravir during recovery from cuprizone-induced demyelination inhibits remyelination. The process of remyelination occurs when mature oligodendrocytes regenerate new myelin sheaths around axons of neurons in the CNS [111, 134]. Remyelination can restore conduction properties to axons leading to restoration of neurological function [111, 134]. There is persistent myelin abnormalities seen in HAND patients, regardless of the administration of cART [108-110]. In order to examine the effect of EVG, on remyelination, we used a widely implemented toxin-induced demyelination model. The copper chelator, cuprizone (bis-cyclohexanone-oxaldihydrazone), is combined into the feed of mice for five weeks, and targets mature oligodendrocytes to die [77, 121, 122], creating a consistent demyelination best seen in the corpus callosum, the largest white matter tract in the mouse brain [77, 121, 122]. In addition, this demyelination is accompanied by the accumulation of microglia and astrocytes [77]. Removal of cuprizone from the feed permits remyelination over the course of three weeks [77, 121, 122] During the three-week recovery period following cuprizone-induced demyelination. EVG/COBI was injected at a dose found to result in similar plasma levels as those reported in human patients [135, 136]. In a separate experiment, we compared two routes of administration of the drug: IV

49

(Intravascular) or IP (Intraperitoneal). Plasma levels resulting from IV injection were closer to the human plasma level (Table 3) [135].

Treatment	Route of administration	Time point	Average Plasma Conc. in µg/ml	N#
DMSO	IP	5 hours	0	2
EVG/COBI	IP	5 hours	5.35	1
DMSO	IV	5 hours	0	3
EVG/COBI	IV	5 hours	13.47	2
DMSO	IP	7 days	0	2
EVG/COBI	IP	7 days	0.19	2
DMSO	IV	7 days	0	3
EVG/COBI	IV	7 days	0.845	2

Table 3: A comparison between IP and IV route of adminstration: mice were treated with the vehicle (DMSO) with or without EVG/COBI daily for 7 days. Plasma samples were taken 5 hours after the injection of drug on day 1 and 7 and analyzed by mass spectometry.

EVG was administered daily via IV jugular vein cannula; COBI was co-administered with EVG in order to boost EVG concentrations, while control animals received the vehicle, DMSO (Figure 9). After 5 weeks of cuprizone feeding or at the end of the three-week recovery period, brains were processed for frozen sections and luxol fast blue (LFB) staining was used to label myelin (Figure 9). The cuprizone-treated mice showed the characteristic

decrease in myelin in the center of the corpus callosum following 5 weeks of cuprizone ingestion and the expected complete remyelination after three weeks recovery (Figure 9). However, mice treated with EVG and COBI during recovery from cuprizone had significantly less myelin compared with mice that remained untreated during the 3 week recovery or mice treated with DMSO during the recovery from cuprizone exposure (Figure 9). Interestingly, there were no gross changes in myelin in the corpus callosum in EVG/COBI-injected mice in the absence of cuprizone when compared with all other control groups (Figure 9).

To further confirm the effect of EVG on remyelination, we stained mouse sections from all experimental groups for the mature oligodendrocyte marker, ASPA [137, 138]. As expected, there were significantly fewer ASPA positive cells in the 5 week cuprizone-exposed mice compared with control mice; after the three-week recovery period, the number of ASPA positive cells in cuprizone exposed mice permitted to recover for 3 weeks were no different from control levels (Figure 10). In contrast, there were fewer ASPA positive cells in the corups callosum of mice treated with EVG/COBI following the 3 week recovery from cuprizone exposure compared with control mice, DMSO-injected cuprizone recovery mice, or untreated cuprizone recovery mice (Figure 10). These data are consistent with LFB data shown in Figure 5 and suggest that EVG inhibits remyelination of the corpus callosum.

While the precise mechanisms of cuprizone-mediated demyelination are unclear, several studies have demonstrated that anti-inflammatory agents can attenuate cuprizone-induced damage to the corpus callosum and prevent

demyelination [139]. To determine whether astrogliosis and/or microgliosis persist during EVG/COBI treatment during recovery from cuprizone treatment, we measured the effect of EVG on the inflammatory environment during remyelination. We stained mouse sections for astrocytes and microglia using GFAP and IBA1, respectively (Figure 11). We observed an increase in GFAP and IBA1 fluorescent intensity in 5 week cuprizone-treated mice which subsequently decreased to the levels of control mice after three weeks of recovery. However, in the EVG/COBI-injected cuprizone recovery mice GFAP and IBA1 fluorescent intensity were still increased when compared with untreated cuprizone recovery and DMSO-injected cuprizone recovery mice (Figure 11).

Our data suggest that EVG inhibits differentiation of OPCs into mature oligodendrocytes *in vitro*. If the same were occurring *in vivo*, we would expect an increase in OPCs or immature oligodendrocytes in the corpus callosum of cuprizone-treated mice receiving EVG/COBI during recovery. To determine whether OPCs were increased in the corpus callosum of mice given EVG/COBI during the 3 week recovery from cuprizone, we stained mouse sections for NG2. Consistent with previous results, we observed an increase in the NG2 fluorescent intensity in 5 week cuprizone-treated mice [140]; however, the increase in NG2 positive was reversed to the level of untreated mice after three weeks of recovery. In contrast, in the EVG/COBI-injected cuprizone recovery mice, NG2 fluorescent intensity was still increased when compared with untreated cuprizone recovery and DMSO-injected cuprizone recovery mice (Figure 12).

The integrated stress response (ISR) partially mediates elvitegravir-driven inhibition of oligodendrocyte maturation, *in vitro*. Previous studies have shown that EVG induces neuronal damage via induction of the ISR [12]. ISR induction is known to halt oligodendrocyte differentation [141]. To determine whether EVG is affecting OPC maturation via ISR induction, , we examined whether ISR inhibitor, trans-ISRIB, alleviated the observed EVG-induced OPC maturation defect *in vitro* [142]*.* Representative images show that cultures pretreated with trans-ISRIB one hour prior to EVG (3.5 µM) treatment had increased immature and mature oligodendrocytes, identified as GalC- and MBP-positive cells, compared with cultures not pretreated with ISRIB (Figure 13A). These observations were confirmed by counting the number of GalC positive immature and MBP positive mature oligodendrocytes in cultures pretreated with trans-ISRIB as compared with cultures not pretreated with trans-ISRIB (Figure 13B,C). Examination of MBP protein expression levels in which cultures were pretreated with ISRIB demonstrated maintenance of MBP protein levels compared with cultures not pretreated with trans-ISRIB (Figure 13D,F). Notably, cultures pretreated with trans-ISRIB prior to EVG (10 µM) treatment, resulted in immature and mature oligodendrocyte numbers and expression of MBP comparable to cultures not pretreated with trans-ISRIB (Figure 13).

2.5 Discussion

The introduction of cART has changed the landscape of HIV/AIDS, viral suppression results in fewer patients progressing to AIDS and expansion of the lifespan of HIV-positive individuals. However, given the persistence of

HAND despite of cART administration, a better understanding of cART side effects is necessary as patients now remain on cART regime for the entirety of their increased lifespans. Specifically, the new class of INSTIs require close examination as their use worldwide continues to grow.

In the present study, we investigated the effects of front line ARV class INSTIs, EVG and RAL, on oligodendrocyte maturation and myelination. Maturation and myelination inhibition was induced only by EVG. Furthermore, our *in vitro* and *in vivo* studies showed EVG activated ISR in oligodendrocytes. Pharmacological attenuation of the ISR with trans-ISRIB, protected against EVG-induced oligodendrocyte maturation inhibition, *in vitro*.

Despite being in the same class of ARV agents, EVG caused dose-dependent inhibition of oligodendrocyte maturation whereas RAL did not. This within-class difference was dramatic as EVG at 3.5 μM and 10 μM induced a 50% and 95% decrease in GalC- and MBP-positive cells, respectively, whereas RAL, at similar doses and time course, had no effect. Moreover, the immunoblot results corroborated the immunocytochemistry as MBP expression was dramatically decreased with 3.5 μM and 10 μM EVG treatment whereas RAL had no effect. These data provide novel, compelling evidence for EVG-induced oligodendrocyte maturation defects. Furthermore, these data add to previous studies showing similar differential effects of INSTIs, EVG and RAL, *in vitro,* albeit in neurons [12, 143]. Importantly, our observations regarding EVG and RAL highlight critical differences in the effects on oligodendrocyte maturation within each ARV class. These studies could be helpful to clinicians when deciding which ARV drug to administer,

especially in younger patients that are still developing myelin and might be on cART for decades.

We utilized the cuprizone demyelination model in order to examine the effects of EVG on remyelination *in vivo*. Cuprizone-induced demyelination is widely utilized to study demyelination/remyelination not caused directly by inflammation, as it leads to the specific degeneration of oligodendrocytes in the corpus callosum [77, 121, 122]. Using this model to demyelinate the corpus callosum, we showed that daily administration of EVG/COBI during the 3-week recovery period, following cuprizone ingestion, resulted in diminished remyelination and decreased mature oligodendrocytes via LFB staining and ASPA positive cell counts, respectively plus an increase in the NG2 positive OPCs which correspond with the *in vitro* finding in which EVG/COBI prevented OPCs from maturation. Notably, there was no change in LFB staining and ASPA positive cell counts in control mice injected daily with EVG/COBI suggesting that EVG induces inhibition of differentiation in OPCs, but has no affect on already mature oligodendrocytes. There are limitations to these data as there could be some additive affect of cuprizone, itself, in EVG/COBI-injected cuprizone recovery mice. Thus, these data need to be interpreted thoughtfully as cuprizone-induced demyelination does not reiterate the white matter loss and abnormalities observed in HAND patients. This findings highlights the need for mouse models of HIV infection that recapitulate HIV persistence in the ART era as well as the myelin irregularities observed in HAND patients [144, 145].

An additional concern about the relevance of these findings is whether the doses of these observed effects with EVG are comparable to the doses observed in patients. Doses were selected to cover a wide range of concentrations relevant to the plasma and CSF concentrations observed in patients [44, 129, 146]. It is still unclear how these doses relate to levels of ARV drugs present in the brain parenchyma and some studies have shown that CSF drug concentrations may not accurately reflect this concentration [147]. As there is a focus on improving CNS penetration of ARV agents, it will become even more important to understand the potential side effects of such drugs at higher concentrations.

In addition to characterizing the effects of EVG and RAL on oligodendrocyte maturation, we identified a potential mechanism that mediates this effect. We have previously shown evidence for ISR activation in neurons and astrocytes of HAND patients as well as in neurons in culture treated with different classes of ARV compounds[12, 31, 118, 148]. Furthermore, there is evidence for ISR activation in oligodendrocytes in other neuroinflammatory disease models such as multiple sclerosis [120, 149, 150]. Since there are multiple kinases by which to activate ISR, we examined the convergent upstream product, pEIF2α. The effects of ISR inhibitor, trans-ISRIB, were dose specific as well. Trans-ISRIB, mediated oligodendrocyte maturation rescue in cultures pretreated with trans-ISRIB, prior to EVG (3.5 µM) treatment whereas pretreatment with trans-ISRIB, prior to EVG (10 µM) did not result in rescue of oligodendrocyte maturation. The effect of EVG at 3.5 µM was reversible, as cells matured following drug removal, with GalC- and MBP-positive cells and MBP protein expression resembling controls after 24 hours. However, the

effect of EVG at 10 µM was not reversible. Taken together, these data suggest the cellular stress induced in oligodendrocyte in response to 10 µM EVG treatment is distinct from 3.5 µM EVG and ultimately the cell may be targeted for death rather than survival, although it is possible that there is more than one mechanism that mediates the differentiation defect of EVG on maturing OPCs. Neither dose of EVG led to detected increase in apoptotic cell death, identified as TUNEL-positive cells. However, after 72 hours treatment with EVG (10 µM) there was a small decrease in cell viability, identified as cells positive for propidium iodide which suggests necrotic cell death.

In summary, these data add to a growing body of evidence that suggest a role for cART-mediated persistence of HAND. Specifically, these data support a role for cART-mediated persistence of white matter abnormalities observed in HAND individuals. Furthermore, we implicate the ISR as a potential contributing pathway in EVG-induced oligodendrocyte maturation defects. In addition to the development of new therapeutics with fewer deleterious side effects, we must consider adjunctive therapies designed to alleviate neuronal dysfunction and preservation of myelin formation and maintenance.

2.6 <u>Figures:</u>
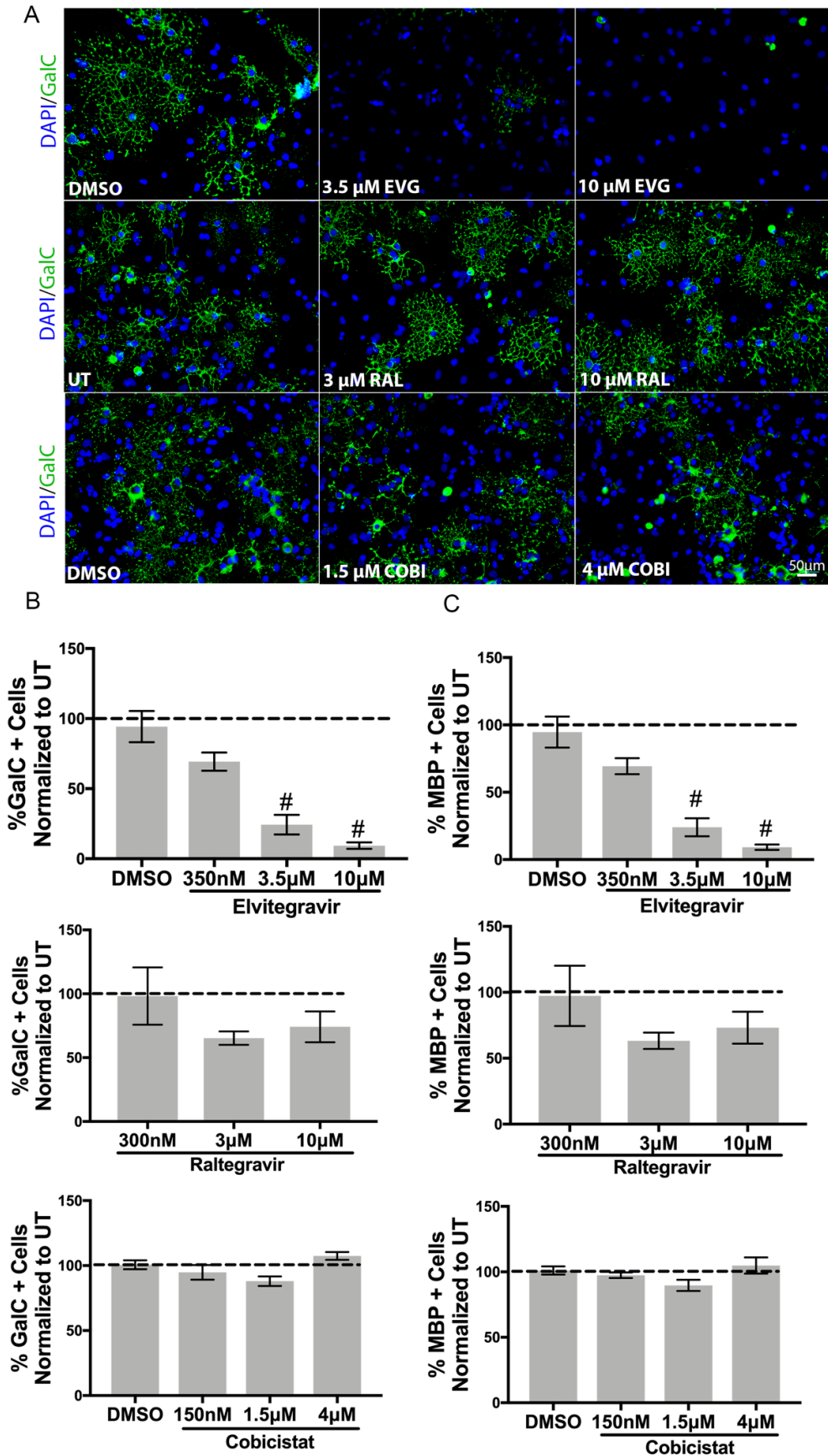
Figure 4: INSTI EVG inhibits oligodendrocyte differentiation, whereas RAL does not. Primary rat cells (OPCs) plated on coverslip were put into differentiation media and treated with vehicle (DMSO), EVG (350nM, 3.5µM, and 10µM), RAL (300nM, 3µM, and 10µM), COBI (150nM, 1.5µM, and 4µM). After 72 hours, cells were fixed and stained with antibody to myelin basic protein (MBP), antibody to galactocerebroside (GalC), and DAPI as shown. A) There was a dose dependent reduction in GalC positive cells in the cells treated with EVG. B) Quantification of the GalC positive oligodendrocytes; significant dose dependent reduction in the GalC positive cells was observed in the EVG treated cells but not RAL nor COBI. C) Quantification of the MBP positive oligodendrocytes; significant dose dependent reduction in the MBP positive cells was observed in the EVG treated cells but not RAL nor COBI. Graphic represent fold changes in MBP and GalC, N=3, one-way ANOVA, # $P<0.0001$.
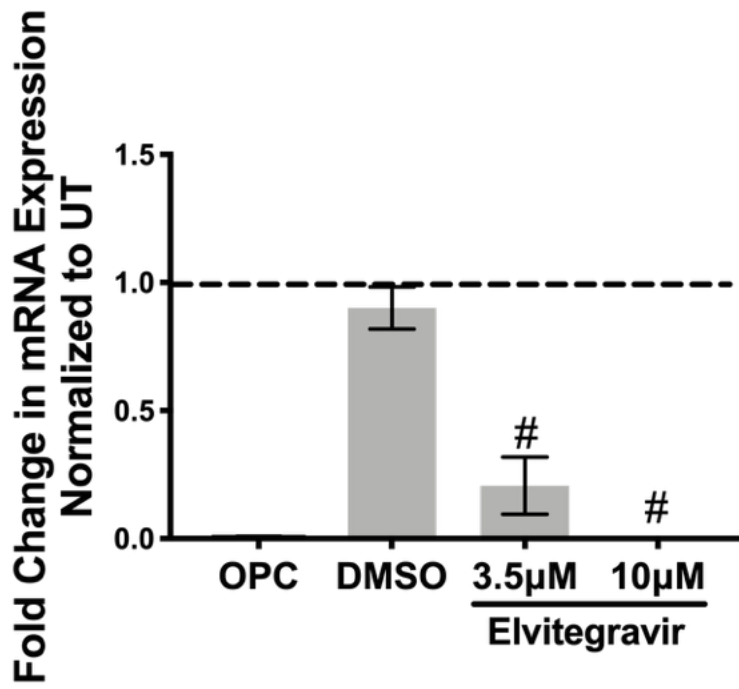
Figure 5: Effect of elvitegravir on MBP mRNA expression. Primary rat cells (OPCs) were put into differentiation media and treated with vehicle (DMSO) without or with elvitegravir at different dosages (3.5µM, and 10µM). A significant dose dependent reduction of mRNA expression level was identified at both 3.5µM and 10µM. One way ANOVA, N=3, # P<0.0001
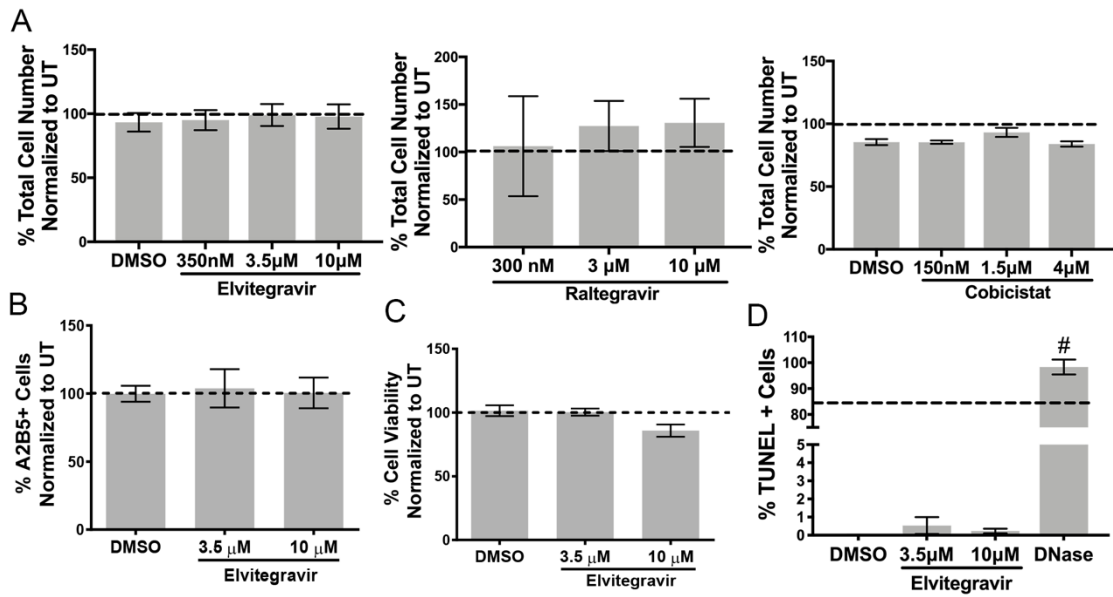
Figure 6: Antiretrovirals do not alter oligodendrocyte precursor cell (OPC) number nor induce apoptosis. Terminal deoxynucleotidyl transferase (TdT) dUTP Nick-End Labeling (TUNEL Assay), cell viability using propidium Iodide, and cell counts using A2B5 and DAPI stains were used to determine if the drugs cause a decrease in the overall number of oligodendrocyte lineage cells. None of the used drugs causes a significant decrease in cell number or an increase in apoptosis. One way ANOVA, N=3, #P<0.0001.
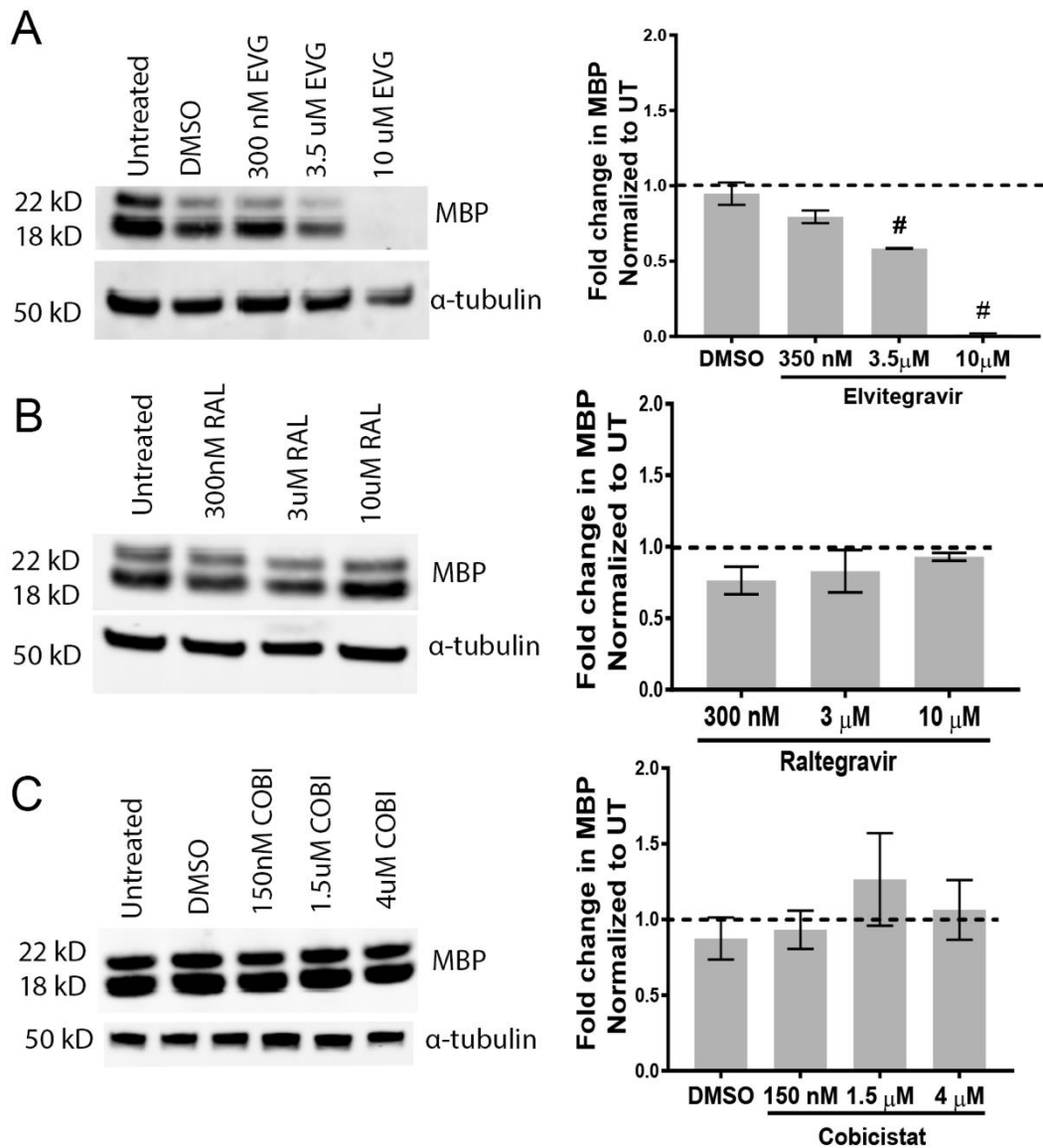
Figure 7: EVG but not COBI or RAL reduces MBP expression levels inoligodendrocytes. Primary rat cells (OPCs) were put into differentiation media and treated with vehicle (DMSO), EVG (350nM, 3.5µM, and 10µM), RAL (300nM, 3µM, and 10µM), COBI (150nM, 1.5µM, and 4µM). After 72 hours, cell lysates were collected in order to measure protein expression. A) Quantification of MBP protein level for OPCs treated with elvitegravir. MBP expression level in untreated cells were compared to cells treated with DMSO with or without EVG at different doses (350nm, 3.5µM, and 10µM). Dose dependent decreases in the MBP protein levels were observed at 3.5µM and 10µM, B) Quantification of MBP protein level of OPCs treated with RAL. MBP expression levels in untreated cells were compared to OPCs treated with DMSO with or without RAL at different doses (300nM, 3µM, and 10µM). No significant reduction was observed in the MBP protein level. C) Quantification of MBP protein level of OPCs treated with COBI. MBP expression levels in untreated cells were compared to OPCs treated with DMSO with or without cobicistat at different doses (150nM, 1.5µM, and 4µM). No significant reduction was observed in the MBP protein level. One way ANOVA, N=3, # $P < 0.0001$

62
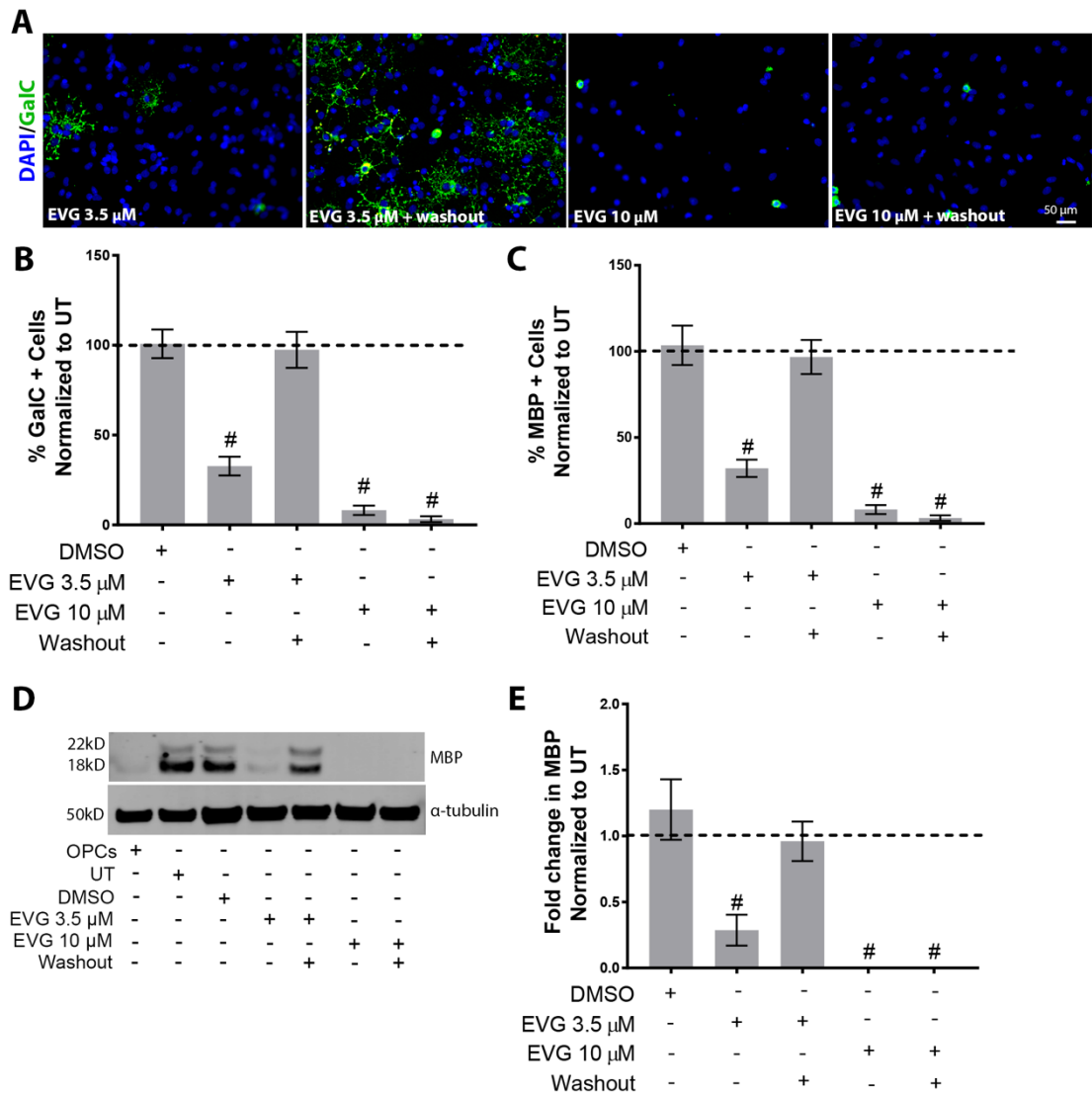
Figure 8: EVG inhibition of differentiation is reversible. A) Oligodendrocyte precursor cells (OPCs) were treated with vehicle (DMSO) and/or EVG (3.5µM, 10µM) at the time of differentiation. After 72 hours, the washout group received new differentiation mediµM without EVG and was allowed to further mature for 24 hours. The cells were fixed and stained for GalC, MBP and DAPI. The inhibitory effect of EVG effects on GalC and MBP expression was reversible at 3.5µM but not 10µM. B) MBP protein level; (OPCs) were treated with vehicle (DMSO) and/or EVG (3.5µM, 10µM) at the time of differentiation. After 72 hours, the washout group received new differentiation medium without elvitegravir and was allowed to further mature for 24 hours. MBP levels were increased following washout in cells treated with 3.5µM elvitegravir but not 10µM. One-way ANOVA, N=3, one-way repeated measures ANOVA, @ P =0.002, & P<0.0001.

A

IV Cannula surgeries
+ drug infusion*

Perfusion

Control Diet |————————————| Weeks
0   5   8

Cuprizone Diet |————————————| Weeks
                      5   8

▬ Control diet
▬ 0.25% Cuprizone diet
* Only DMSO and ART groups recieved IV cannula

B

5 week | **5 week + 3 week recovery or treatment**

Control

Cuprizone

UT | DMSO | EVG+COBI
UT | DMSO | EVG+COBI

400um

C

5 week Control	+	+	+	+	−	−	−	−
5 week Cuprizone	−	−	−	−	+	+	+	+
3 week Untreated	−	+	−	−	−	+	−	−
3 week DMSO	−	−	+	−	−	−	+	−
3 week EVG/COBI	−	−	−	+	−	−	−	+
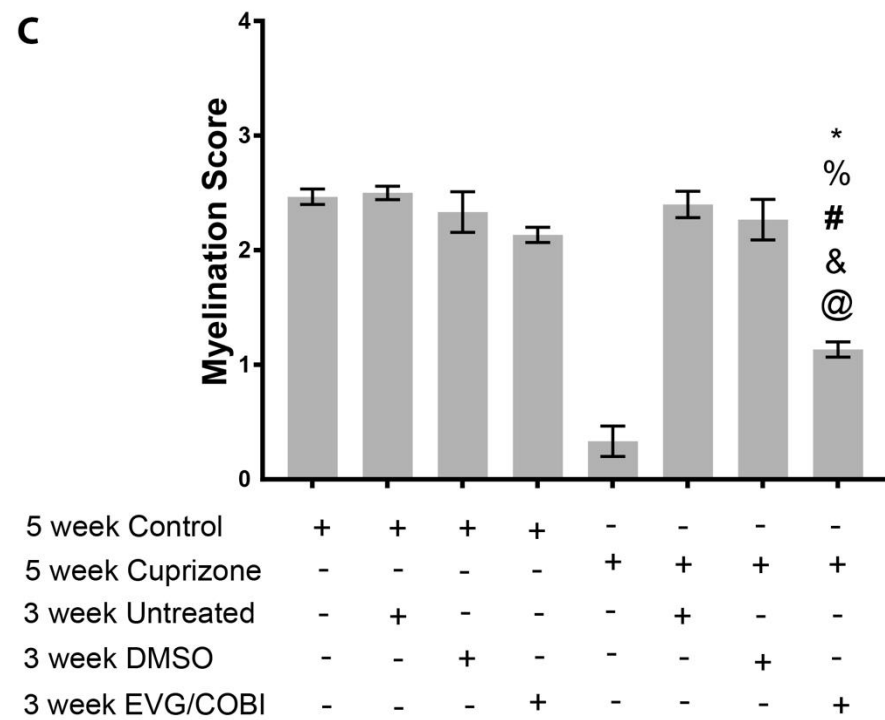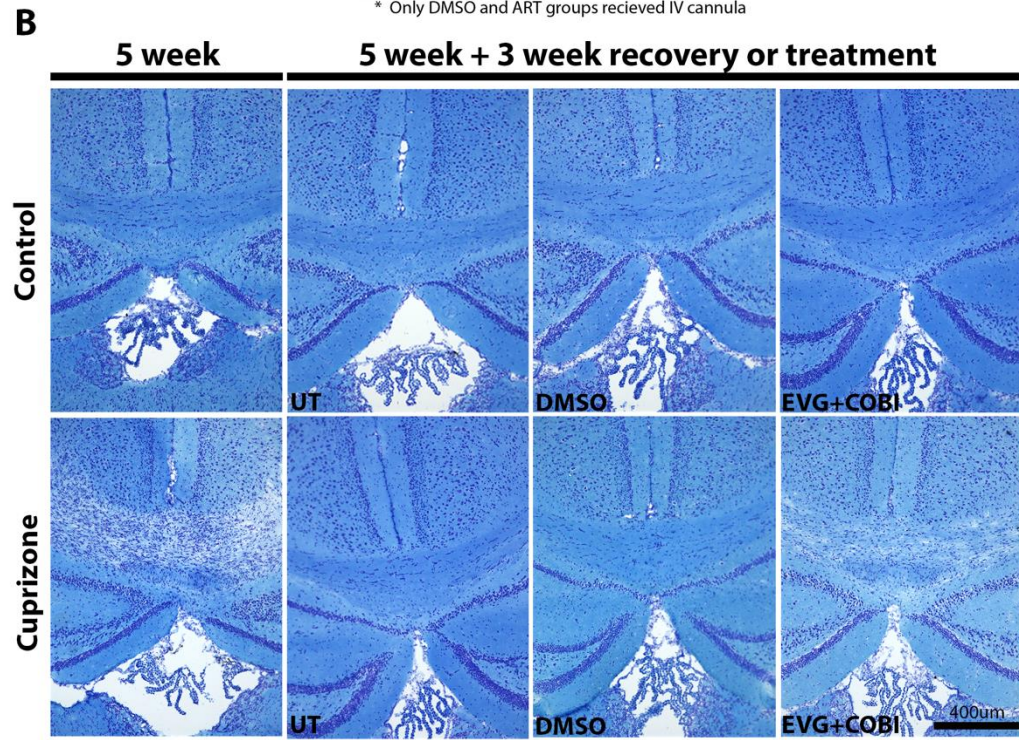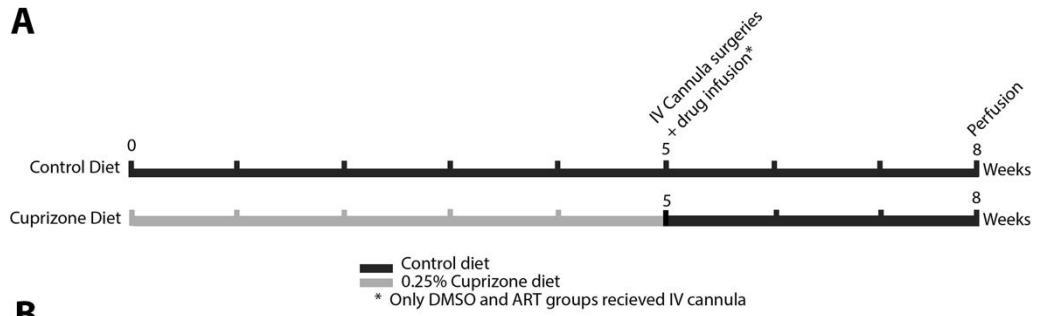
Figure 9: <u>EVG inhibits remyelination in the cuprizone model of demyelination/remyelination.</u> Six to eight week old C57BL/6 female mice were divided into two groups. The 1st group received control diet throughout the whole experiment, the 2nd group received 0.25% cuprizone in their diet for the 1st 5 weeks of the experiment then control diet without cuprizone for a three week recovery period. Within each of these groups, subgroups were as follows: mice euthanized at 5 weeks to see the lesion, mice with or without cuprizone for 5 weeks and no other additives at the 8 week time point, mice given the vehicle DMSO for the 3 week recovery period, mice given elvitegravir/cobicistat in DMSO for the 3 week recovery period. Luxol Fast Blue (LFB) staining was performed on cryopreserved brain sections at the level of the corpus callosum.The lesion in the corpus callosum is clearly visible in the 5 week cuprizone group as compared with controls. This lesion is remyelinated after three weeks. However, the group of mice that were fed cuprizone and then received EVG/COBI during the 3 weeks recovery continued to exhibit a lack of myelin when compared to the other group. Semi-quantification of demyelination by blind examiner scoring (3= intact myelin and 0=complete demyelination).[140, 151] . One way ANOVA, N=5, @ CUPZ ART compared to 5 Week CTL $p = < 0.0001$, & Cupz ART Compared to 8 Weeks CTL $p = < 0.0001$, # Cupz ART compared to CTL DMSO $p = < 0.0001$, % Cupz ART compared to CUPZ UT $p = < 0.0001$, *CUPZ art compared to CUPZ DMSO $p = < 0.0001$
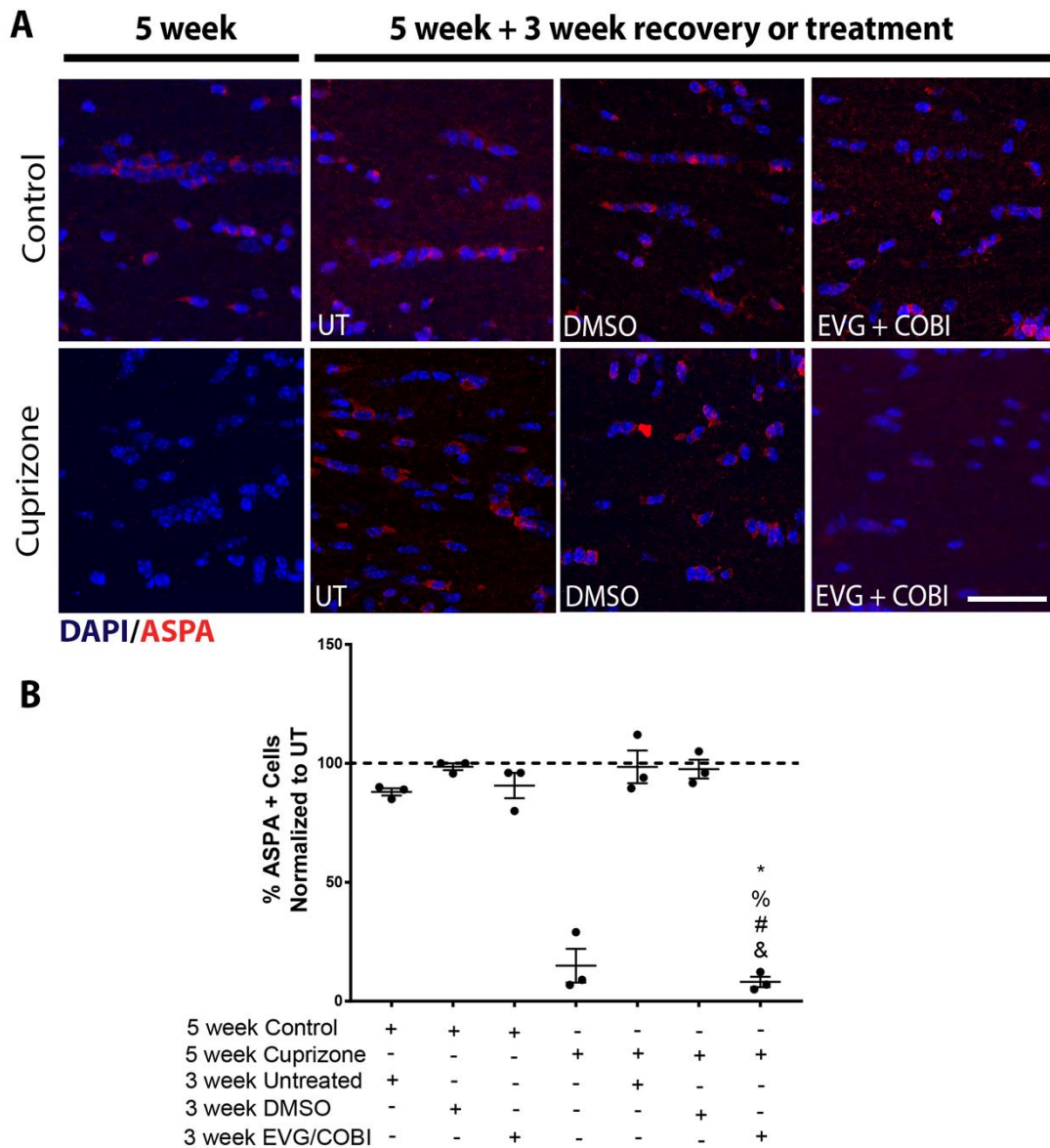
Figure 10: ASPA positive oligodendrocytes remain decreased in animals after 3 weeks of EVG treatment during recovery from cuprizone intoxication as compared with cuprizone-only treated animals. Six to eight week old C57BL/6 female mice were divided into two groups. The 1st group received control diet throughout the whole experiment, the 2nd group received 0.25% cuprizone in their diet for the 1st 5 weeks of the experiment then control diet without cuprizone for a three week recovery period. Within each of these groups, subgroups were as follows: mice euthanized at 5 weeks to see the lesion, mice with or without cuprizone for 5 weeks and no other additives at the 8 week time point, mice given the vehicle DMSO for the 3 week recovery period, mice given elvitegravir/cobicistat in DMSO for the 3 week recovery. Cryosections of mouse brain at the level of the corpus callosum were stained with antibody to ASPA which labels oligodendrocyte cell bodies. The number of the ASPA positive cells were normalized to DAPI positive cells. There were no significant differences between the group of mice received normal diet plus EVG with the group of mice received normal diet or normal diet plus vehicle. The group of mice received cuprizone in their diet followed by EVG during the recovery period showed a significant reduction in the number of ASPA

positive cells when compared to mice had cuprizone in their diet then normal diet or normal diet plus vehicle during the recovery period. One way ANOVA, N=3, & Cupz ART Compared to CTL UT p = < 0.0001, # Cupz ART compared to CTL DMSO p = < 0.0001, % Cupz ART compared to CUPZ UT p = < 0.0001, * CUPZ art compared to CUPZ DMSO p = < 0.0001
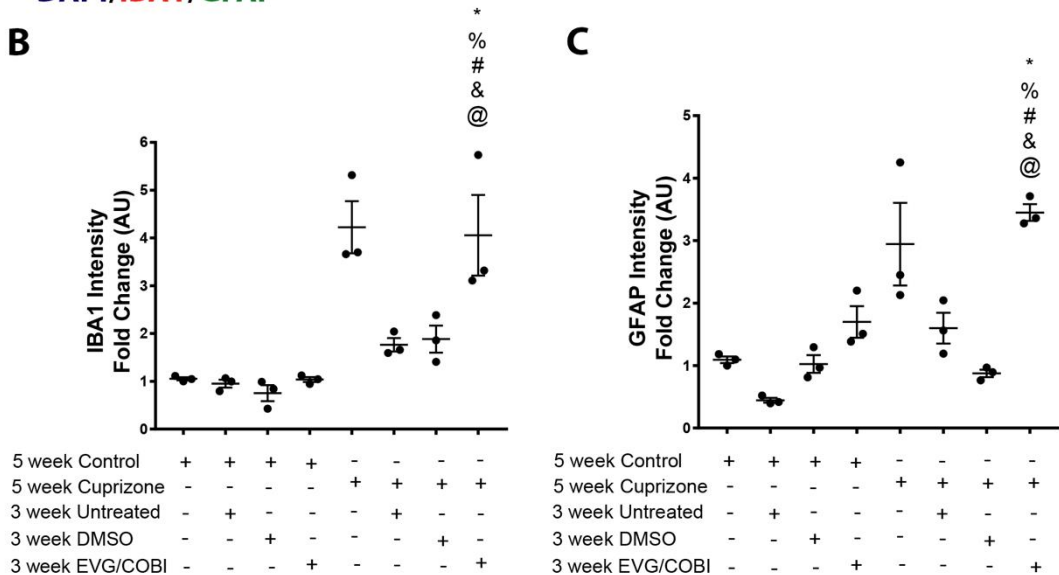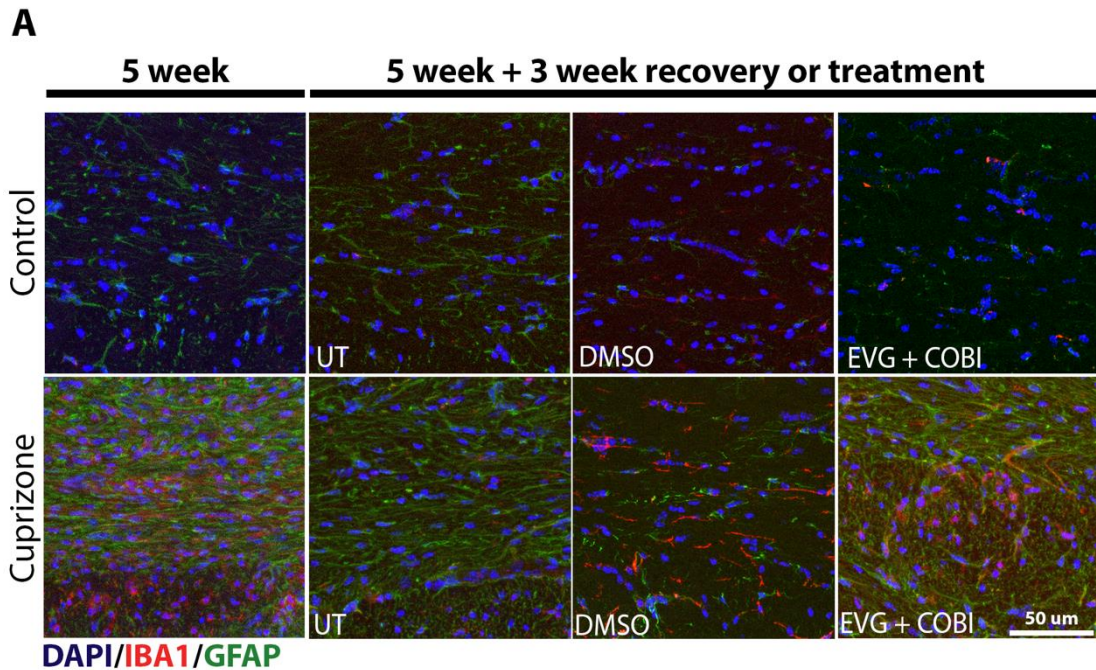
A

5 week | 5 week + 3 week recovery or treatment

Control

Cuprizone

DAPI/IBA1/GFAP

50 um

UT | DMSO | EVG + COBI

B

5 week Control	+	+	+	+	-	-	-	-
5 week Cuprizone	-	-	-	-	+	+	+	+
3 week Untreated	-	+	-	-	-	+	-	-
3 week DMSO	-	-	+	-	-	-	+	-
3 week EVG/COBI	-	-	-	+	-	-	-	+

C

5 week Control	+	+	+	+	-	-	-	-
5 week Cuprizone	-	-	-	-	+	+	+	+
3 week Untreated	-	+	-	-	-	+	-	-
3 week DMSO	-	-	+	-	-	-	+	-
3 week EVG/COBI	-	-	-	+	-	-	-	+

Figure 11: EVG treated mice have glial activation in the corpus callosum. Six to eight week old C57BL/6 female mice were divided into two groups. The 1st group received control diet throughout the whole experiment, the 2nd group received 0.25% cuprizone in their diet for the 1st five weeks of the experiment then control diet without cuprizone for a three week recovery period. Within each of these groups, subgroups were as follows: mice euthanized at 5 weeks to see the lesion, mice with or without cuprizone for 5 weeks and no other additives at the 8 week time point, mice given the vehicle DMSO for the 3 week recovery period, mice given EVG/COBI in DMSO for the 3 week recovery. (A) Labeling for astrocytes (GFAP) and microglia (IBA1) shows an increase in both in the 5 week cupiraozne group and the group treated with EVG/COBI during the recovery period. (B) This was analyzed by intergrated intensity measurements. N=5, one-way ANOVA, for GFAB; @CUPZ ART compared to 5 Week CTL p = 0.004, & Cupz ART Compared to CTL 8 Weeks CTL p = < 0.0001, #Cupz ART compared to CTL DMSO p = 0.0003, %Cupz

ART compared to CUPZ UT p = 0.0036, * CUPZ art compared to CUPZ DMSO p = 0.0001. For IBA1; @Cupz ART Compared to CTL 5 wks, p = 0.0003, & Cupz ART Compared to 8 weeks CTL p = 0.0002, # Cupz ART Compared to CTL DMSO p = 0.0001, %Cupz ART Compared to CUPZ UT p = 0.0037, *Cupz ART Compared to CUPZ DMSO p = 0.0057
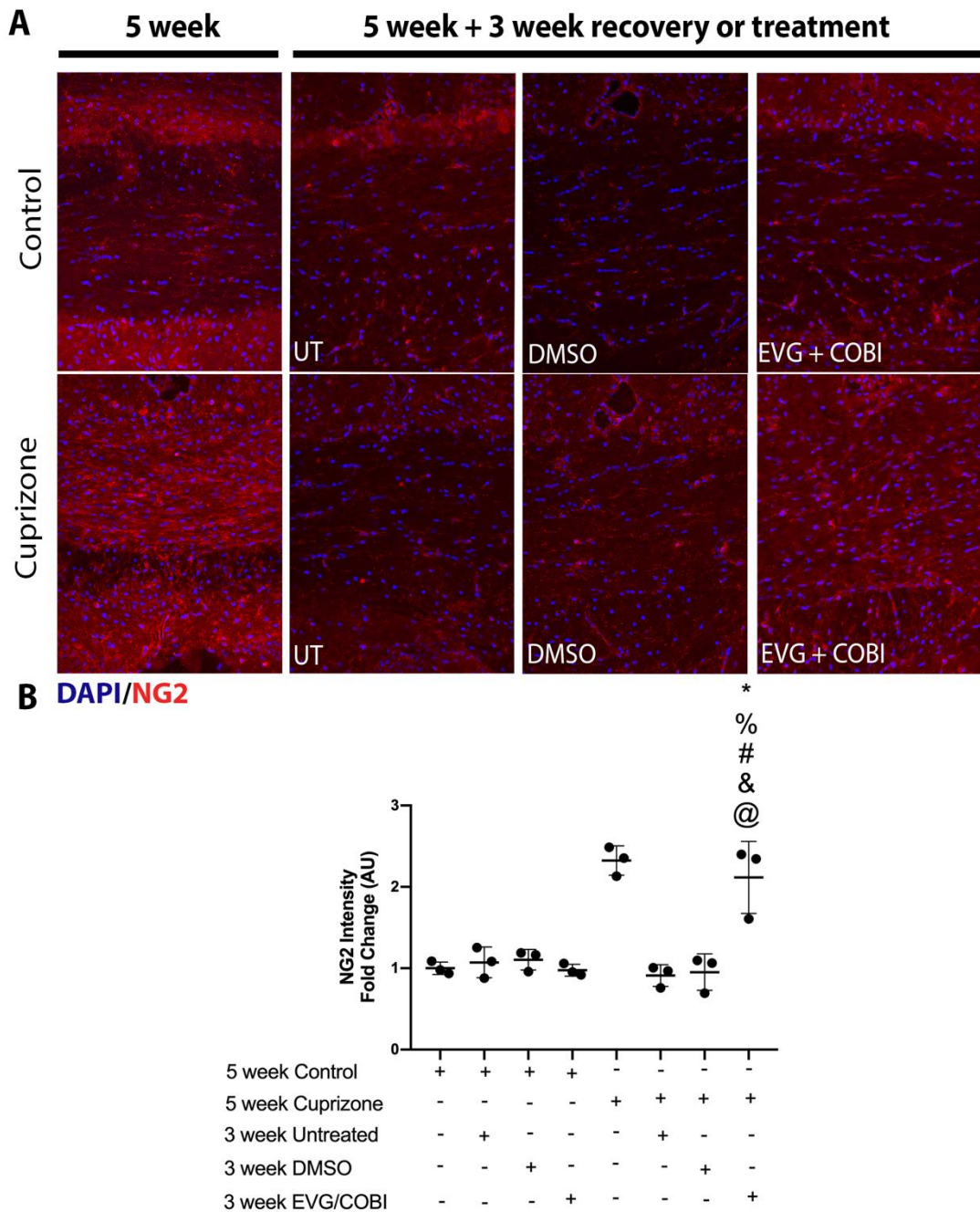
Figure 12: EVG treated mice shows an increase in NG2 positive OPCs in the corpus callosum. Six to eight-week-old C57BL/6 female mice were divided into two groups. The 1st group received control diet throughout the whole experiment, the 2nd group received 0.25% cuprizone in their diet for the 1st five weeks of the experiment then control diet without cuprizone for a 3 weeks recovery period. Within each of these groups, subgroups were as follows: mice euthanized at 5 weeks to see the lesion, mice with or without cuprizone for 5 weeks and no other additives at the 8 weeks, mice given the vehicle DMSO for the 3 weeks recovery period, mice given EVG/COBI in DMSO for the 3 weeks recovery. An integrated intensity shows a sustained increase in the NG2 positive OPCs in the EVG/COBI-injected cuprizone recovery mice compared with untreated cuprizone recovery and DMSO-injected cuprizone

recovery mice. ANOVA, N=3, one-way ANOVA, @ EVG/COBI injected cuprizone compared to 5 weeks control P<0.0001, & EVG/COBI injected cuprizone compared to control DMSO P=0.0002, # EVG/COBI injected cuprizone compared to control injected EVG/COBI P<0.0001, % EVG/COBI injected cuprizone compared to DMSO injected cuprizone P<0.0001, * EVG/COBI injected cuprizone compared to 8 weeks recovery P<0.0001.
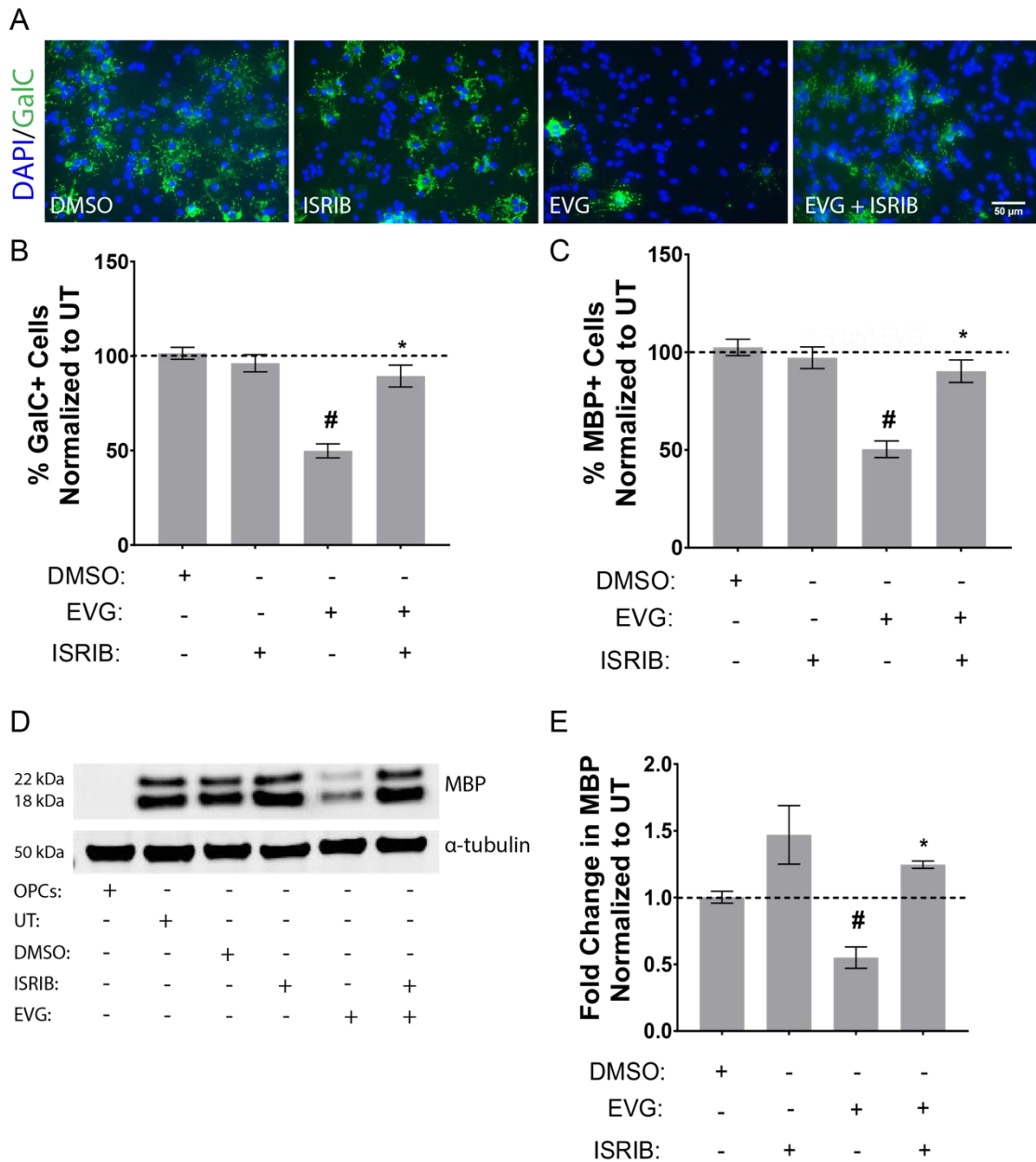
Figure 13: An eIF2α inhibitor (TRANS-ISRIB) rescued oligodendrocytes maturation in cells treated with EVG in-vitro. Primary rat cells (OPCs) plated on coverslip were put into differentiation medium and treated with vehicle (DMSO), Elvitegravir 3.5µM with or without TRANS-ISRIB. After 72 hours in differentiation medium, cells were fixed and stained with antibodies to GalC and MBP as well as DAPI as shown in A). B) Significant increase in the number of GalC positive cells was noted when cells were treated with elvitegravir plus TRANS-ISRIB at 3.5µM compared to cells treated with elvitegravir without TRANS-ISRIB. C) Significant increase in the number of the MBP positive cells was noted when cells were treated with elvitegravir at 3.5µM when compared to cells treated with elvitegravir without TRANS-ISRIB. D) TRANS-ISRIB rescued MBP protein levels in cell treated with elvitegravir at 3.5µM, the result was normalized to loading control and to the untreated group, one-way repeated measures ANOVA, N=3, one way ANOVA, # P <0.05.

CHAPTER3: Effects of HIV anti-retroviral drugs on oligodendrocyte differentiation via the SREBP1 pathway:

3.1 <u>Abstract:</u>

Despite effective viral suppression and decreased mortality rate through combined antiretroviral therapy (cART), approximately half of HIV-positive patients on ART have HIV-associated neurocognitive disorder (HAND). A consistent finding revealed in studies of antiretroviral-treated HIV-positive patients is persistent white matter and myelin abnormalities. Myelin is the plasma membrane of oligodendrocytes and is crucial for rapid signal transduction and axonal maintenance of central nervous system (CNS) axons. A reduction in the amount of myelin contributes to neurocognitive dysfunction. Our lab has shown that differentiation of oligodendrocyte precursor cells (OPCs) is negatively affected by ART, but the mechanism behind this is still not clear. In this study we focused on RIT, a protease inhibitor used in conjunction with other drugs to improve pharmacokinetics of the compound. In the plasma, it increases the levels of both triglycerides and cholesterol due to increasing both fatty acid and cholesterol synthesis in the adipose tissue of the liver by activating a master lipid metabolism gene: the sterol regulatory element-binding protein (SREBP). Additionally, it has been shown that SREBP1 plays a major role in differentiation of oligodendrocytes and inhibiting SREBP activation results in a significant reduction in the number of mature oligodendrocytes in a differentiation paradigm *in vitro*. We hypothesize that changes in oligodendrocyte maturation due to RIT, are regulated by the SREBP1 pathway. We investigated both SREBP1 and three lipid enzymes in oligodendrocytes treated with RIT using an in-vitro model of primary

oligodendrocyte precursor cells from rats to understand the mechanism by which RIT inhibits oligodendrocyte differentiation. Our data show that treatment of oligodendrocyte progenitor cells in culture with RIT at the point of differentiation increased protein levels of SREBP1 and increased protein levels of Fatty Acid Synthase, a precursor for palmitate synthesis. Mass Spectometry of cell lysates reveals an increase in both newly made cholesterol and newly made palmitate in the RIT treated cells. These findings suggest that SREBP pathway is important regulator for oligodendrocyte maturation and that disruption of their activity may affect oligodendrocytes maturation myelination.

3.2 <u>Introduction:</u>

Cerebral white matter consists largely of densely packed oligodendrocytes that myelinate the neuronal axons. Oligodendrocytes are one of four glial cells present in CNS and form 5-8% of the total glial cells in the CNS[92]. These cells produce myelin, the lipid sheath that wraps and insulates axons and serves to increase the conductivity of the electrical impulses. The myelin membrane is apoprximately 70% lipid and during maturation and myelination, oligodendrocytes elaborate tremendous amounts of cellular membrane highly enriched in lipids. In addition, multiple proteins specific for myelin such as proteolipid protein (PLP) and myelin basic protein (MBP) are also generated and have their specific locations among the lipids in the myelin membrane [152]. One of the regulators of lipid metabolism in cells is Sterol Regulatory Element-binding Proteins (SREBPs) family (Figure 14). SREBPs are basic helix-loop-helix-leucine zipper transcription factors. The SREBP family is a

master regulator of cellular lipid metabolism, composed of three subgroups, SREBP1a, SREBP1c and SREBP2. In general, SREBP1a is important activator of all SREBP genes, involving synthesis of cholesterol, fatty acids, and triglycerides. While, SREBP1c is required for fatty acid synthesis and SREBP2 governs expression of enzymes that regulate synthesis of cholesterol. SREBP proteins are synthesized in the endoplasmic reticulum as a precursor protein. Various stimuli such as the cellular concentration of sterol regulate the cleavage of the membrane-bound precursor to be released as the mature nuclear form. The SREBP cleavage activating protein (SCAP), another ER membrane-embedded protein binds to SREBP at low concentration of cholesterol and transports it to Golgi apparatus. However, when cholesterol levels are high, oxysterol-binding Insigs (Insulin induced gene) induce a tight interaction with cholesterol-binding SCAP and prevent movement of the SREBP/SCAP complex to the Golgi blocking SREBP processing and activity [153, 154]. We have previously shown that SREBP is important for the differentiation of oligodendrocytes from the precursor stage to the mature stage and inhibition of SREBP transport to the nucleus inhibited process extension and expression of MBP [11, 85]. We hypothesize that oligodendrocytes treated with RIT induce SREBP expression leading to increased levels of cholesterol and fatty acids in these cells[155] and this impalance in cholesterol and fatty acids, in turn, inhibits differentiation of oligodendrocytes.

3.3 <u>Material and Methods:</u>

All experiments were performed following the guidelines set by Children's Hospital of Philadelphia Institutional Animal Care and Use Committee (IACUC) and University of Pennsylvania Institutional Animal Care and Use Committees.

Chemical Reagents:

Mouse monoclonal anti-α-tubulin antibody (T5168), biotin, dimethyl sulfoxide (DMSO), fast green FCF, insulin, protease inhibitor cocktail, thyroxine (T4) from (Sigma Aldrich, St. Louis, MO). (Jackson Immunoresearch Laboratories, West Grove, PA): FITC- conjugated goat anti-mouse IgG3, Rhodamine-conjugated goat anti-rat IgG. (LiCOR, Lincoln, NE): Odyssey goat antimouse IRdye 800CW, goat antimouse IRdye 680RD, goat antirat IRdye 800CW, goat antirat IRdye 680RD, goat anti- rabbit IRdye 800CW, and goat antirabbit IRdye 680RD were from (Jackson Immunoresearch Laboratories, West Grove, PA). (Chemicon International, Temecula, CA) provided mouse monoclonal anti- glyceraldehyde 3-phosphate dehydrogenase antibody (GAPDH, MAB374). (Covance Laboratories, Conshohocken, PA) provided mouse monoclonal anti-MBP (SMI-99). B27 supplement, 4%– 12% Bis-Tris gradient gels, Dulbecco's modified Eagle's medium (DMEM), DMEM/F12, deoxyribonuclease 1 (DNase), Ham's F12, L-glutamine, Hank's balanced salt solution, neurobasal medium, and penicillin/streptomycin were from Life Technologies (Carlsbad, CA). (R&D Systems, Minneapolis, MN) was the source of basic fibroblast growth fac- tor (bFGF) and platelet-derived growth factor -AA (PDGF-AA). (Roche Diagnostics, Basel, Switzerland) supplied biotin-16- dUTP. Vectashield with 4',6-diamidino-2-phenylindole (DAPI) was

from (Vector Laboratories, Burlingame, CA). anti-galactocerebroside mouse hybridoma supernatant (GalC H8H9), [131] anti-GFAP mouse hybridoma supernatant, anti-MBP rat hybridoma supernatant (gift of Virginia Lee, University of Pennsylvania, Philadelphia, PA). SREBP1, and HMGCR from (Santa Cruz Biotechnology, Dallas, TX), FASN and ACC from (Cell signaling, Danvers, MA).

Primary cerebral cortex oligodendrocytes cultures

Primary oligodendrocytes precursor cells (OPCs) were collected from post-natal day 1 rats (Sprague Dawley rats, Charles River Laboratories, Malvern, PA) with modification of the previously published techniques.[119] To purify the oligodendrocytes cultures, a shake-off technique was performed at 7-8th day following the prep. For the shake-off procedure, T75 flasks were placed in the shaker incubator at 250 rpm overnight. The following day, cells were filtered through 20μM nylon filter (Merck Millipore, Darmstadt, Germany), followed by 5 minute centrifugation at 1500 rpm. The supernatant was discarded and the pellet resuspended into 5ml of neurobasal medium and incubated in bacteriological petri dish for 15 minutes at 37C° and 5% CO_2, then centrifuged again at 1500rpm for 5 minutes to collect the medium, and the pellets are placed into growth medium. After purification, OPCs were grown using neurobasal medium with B27 with the addition of growth factors including bFGF, PDGF-AA, and neurotrophin-3 (NT3) till reach 70-75% confluency. TO differentiate the OPCs ot mature oligodendrocytes, growth factors were removed and thyroid hormone was added

Western Blot:

Whole cell extracts used to determine the level of the protein of interest, cells were harvested in cold 25 mM Tris (pH 7.4), 1 mM EDTA, 1% SDS, 1% Triton X-100, 150 mM NaCl containing protease and phosphatase inhibitor cocktails (PIs; Roche Diagnostics), sonicated and then centrifuged 30 min at 15,000 rpm. Protein concentration were determined by absorbance using spectrophotometer ND-1000 from Thermo Scientfic (Philadelphia, PA). Ten micrograms of protein were loaded into each lane in the gel. A broad-spectrum molecular weight ladder (Precision Plus Protein, CA) was run on each gel. After separation, proteins were transferred onto Millipore Immobilon-FL membranes and blocked in PBS with 0.1% Tween-20 (PBST) and 5% milk for 20 minutes at 4 °C. Membranes were incubated overnight at 4 °C with primary antibodies in PBST + 5% milk. Primary antibodies to the following antigens were used: MBP (SMI-99, dilution 1:1000), p-eIF2α (1:1000), total eIF2α (1:1000). Loading controls were obtained by using α-tubulin (1:1000 dilution). Membranes were visualized using an Odyssey Infrared Imaging System (LiCOR).

Mass Spectrometry:

Oligodendrocytes primary rat cells were treated for 1 hour and 7 hours with 3 µM RIT or the vehicle DMSO with sodium A Acetate (1-13 C 99%) for labeling at concentration of 1000µM,[156]. The samples were processed at Smilow Center of the University of Pennsylvania.

Statistical analysis:

All data are expressed as mean with SEM. Data were analyzed with Prism 8 (GraphPad Software). Differences between groups were assessed using one-way ANOVA (Unpaired).

3.4 Results:

RIT is a member of the protease inhibitor class of antiretroviral drugs. It acts on the late stage of viral replication resulting in an immature virus that can't infect intact cells [157]. RIT is among the oldest antiretroviral drugs, but remains in use today as a booster to enhance the pharmacokinetics of other antiretroviral drugs due to its inhibition of cytochrome P450 in the liver and intestine[14, 158-160]. Interestingly, individuals on RIT showed a decrease in HDL (High density lipoprotein), cholesterol level and an increase in total cholesterol level, LDL (Low density lipoprotein), and triglyceride levels [161]. We have previously shown a decrease in the number of differentiated oligodendrocytes and myelin proteins when oligodenodrocyte precursor cells (OPCs) were treated with RIT during a differentiation paradigm, but the mechanism behind this effect is still unknown[11]. We placed oligodendrocyte progenitor cells in differentiation medium with or without RIT and performed western blotting for SREBP1c protein after 72 hours. Our results show that the amount of the SREBP1c protein expression is elevated when OPCs were treated with 3µM RIT for 2 hours and 24 hours (Figure 15).

We measured levels of three key enzymes in the lipid synthetic pathway, fatty acid synthase (FASN), acetyl co-A carboxylase (ACC) and 3-hydroxy-3-methyl-glutaryl-coenzyme A reductase (HMGCR). We saw a significant

increase in the protein expression level of FASN at 24 and 72 hours in RIT treated cells compared with vehicle treated OPCs, but no significant difference was noticed for HMGCR or ACC (Figure 16). We then measured the accumulation and de novo synthesis of palmitate and cholestrol using mass spectrometer. The palmitate is an intermediate compound in the synthesis pathway of many sterols . Our results show around 50% increase in the newly synthesized cholesterol and palmitate in OPCs treated with 3μM RIT in concert with differentiation medium for 72 hours, and labeled with ^{13}C acetat for the last 24 hours (Figure 17).

3.5 Discussion:

SREBPs are important regulators for cellular lipogenesis and lipid homeostasis but their role in oligodendrocyte myelination is not well-understood. We have previously shown that treatment of oligodendrocyte progenitor cells with the protease inhibitor RIT resulted in an inhibition of differentiation but we did not identify a mechanism. It is known that RIT increases sterol synthesis by increasing SREBP1 expression in the liver and adipose tissue and sinc the myelin membrane is 70% lipid, we hypothesized that SREBP1 might also be increased in oligodendrocytes upon RIT treatment. The present study suggests that SREBP levels can be dysregulated when oligodendrocyte differentiation is decreased. Since generation of the myelin membrane with proper placement of lipids and proteins is necessary for process extension, it is possible that the alterations in balanced lipids in oligodendrocyte membranes caused by RIT resulted in a reduction in the total number of differentiated cells. The preservation of proper

cell membrane fluidity is important for diffusion of membrane components including different lipids and proteins and is necessary for the dynamics and function of membrane proteins. The alteration in lipid synthesis was identified on the level of the transcription factor SREBP1, in a key enzyme necessary for synthesis of the lipids and in the end product lipids themselves suggesting that an excess of SREBP1 caused by RIT treatment resulted in an alteration in the cells membrane normal dynamics and functions [162]. Our lab published previously that inhibiting SREBPs protein through S1P inhibitor resulted in a significant reduction in the maturation in the oligodendrocytes maturation [13]. Our current study suggests that a balanced amount of SREBP is required for normal maturation of oligodendrocytes. In conclusion, we show that SREBPs could play an important role in oligodendrocyte maturation and myelination. Inhibition or induction of SREBP may prevent process extension, and cellular maturation. All these effects may contribute to impaired myelin packing in the membrane.

3.6 Figures
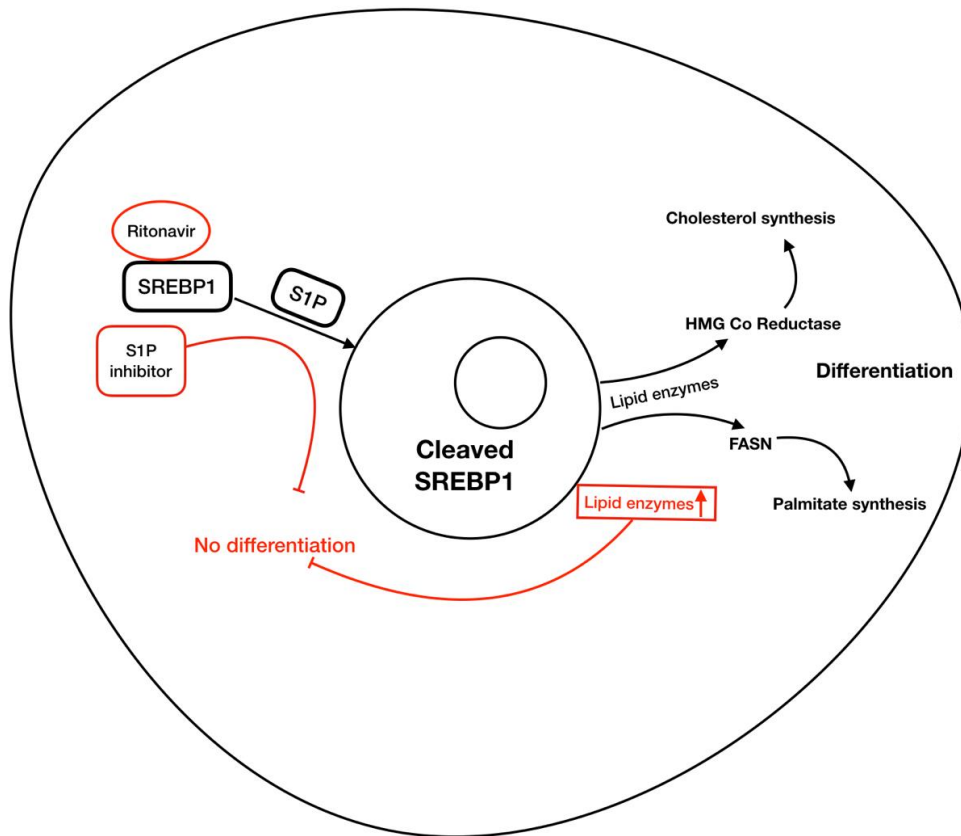
Figure14: Lipid enzymes in oligodendrocytes. reduction or elevation in the lipids enzyme in oligodendrocytes will result in disruption in the harmony in the process of cell membrane extensions.
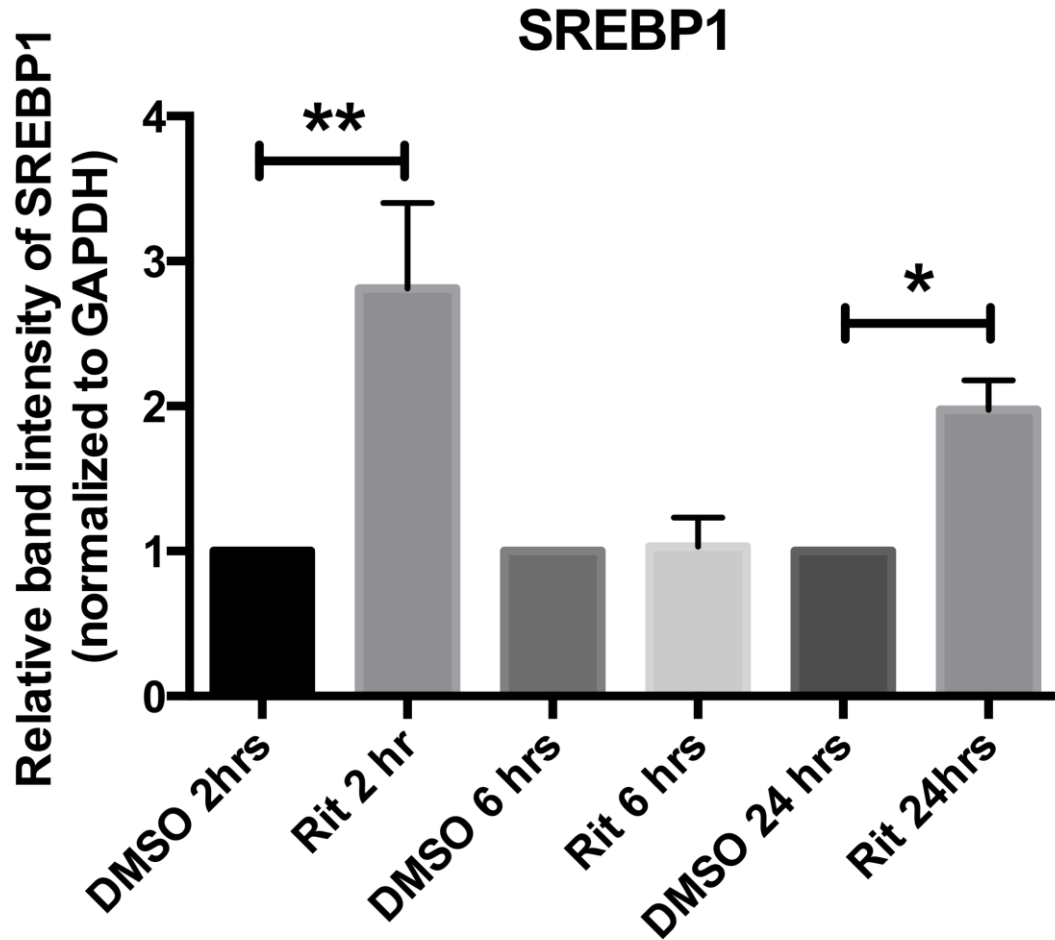
Figure 15: SREBP1 expression is increased at 2 and 24 hours after ritonavir treatment. Western blot measuring SREBP1 protein level at three different time intervals, 2hours, 6hours and 24hours shows a significant increase in SREBP1 level in the group treated with Ritonavir at 2 and 24 hours when compared to the group treated with vehicle (DMSO). N=3, One Way ANOVA, * P<0.05, **P<0.001
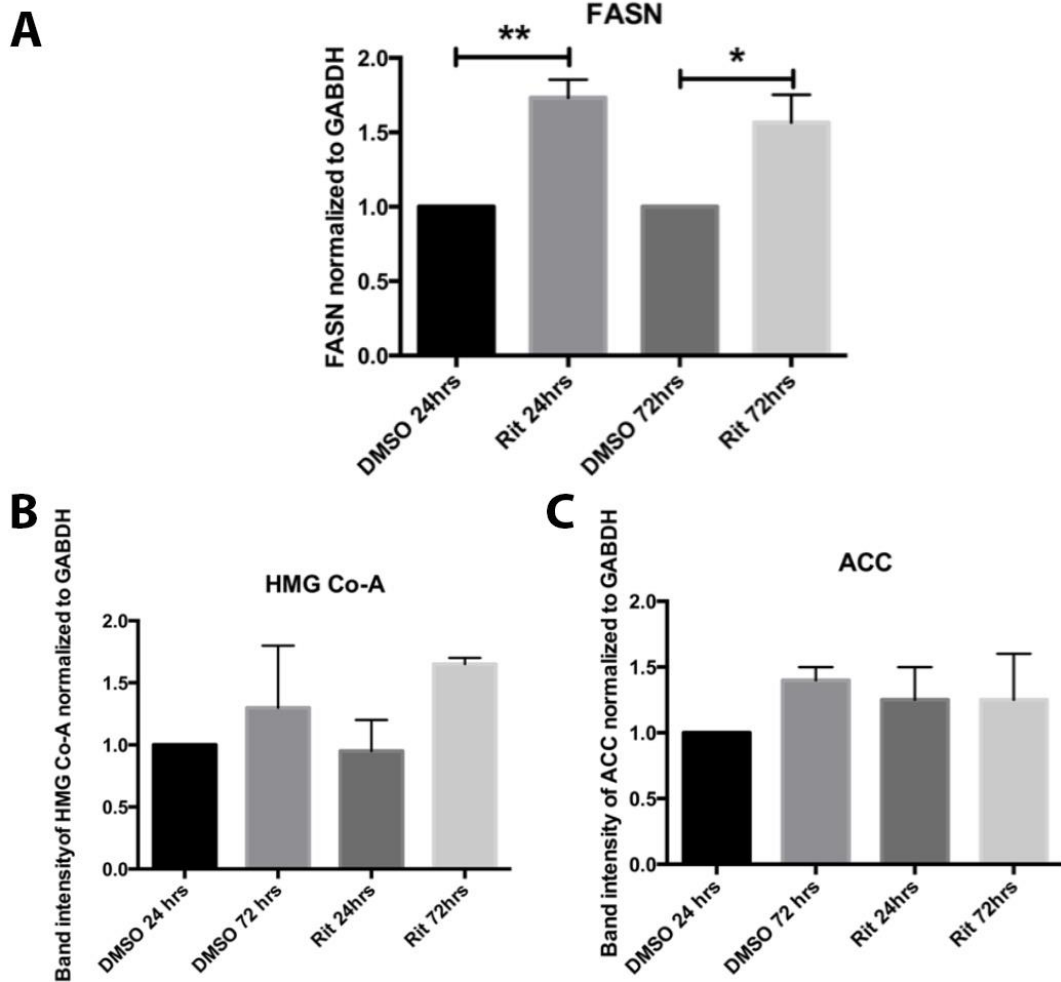
Figure 16: Ritonavir treatment of OPCs significantly ncreased expression of FASN but not ACC or HMGCoAR. Western blot measuring lipid enzymes in differentiated oligodendrocyte precursor cells; A) a significant increase in the FASN protein level when treated with Ritonavir at both 24 and 72 hours compared to OPCs treated with vehicle (DMSO), B,C) there were no significant difference at protein level of both ACC or HMG Co-A when treated with Ritonavir compared to OPCs treated with vehicle. N=3, One Way ANOVA, * P<0.05, **P<0.001
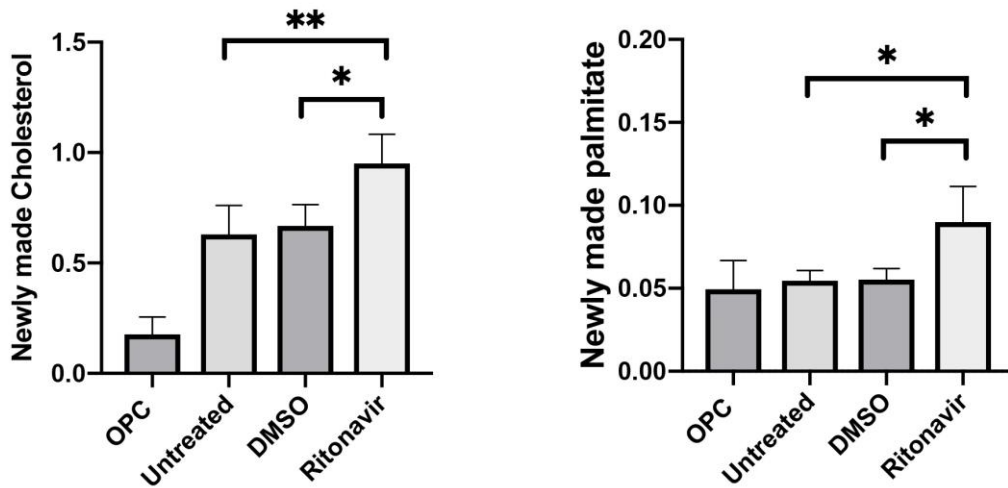
Figure 17: Ritonavir increased levels of newly synthesized palmitate and cholesterol. OPCs treated with DMSO (vehicle) with or without 3µM of ritonavir for three days, ^{13}C acetate was added to the differentiation media for the last 24 hours of treatment. Both newly-made palmitate and cholesterol are increased in cells labeled with acetate compared to DMSO-treated or untreated groups.N=3, * P<0.05,** P<0.01

CHAPTER 4: Discussion and Future Directions

ART plays a major role in the attenuation of viral replication and boosts immune system recovery, but still we see that treatment results in adverse side effects, including cellular impairments which may contribute to the continued incidence and progression of HAND [25, 29, 32, 163-166]. We anticipate that some classes of ART drugs are involved in inhibiting the differentiation of oligodendrocytes using one or multiple pathways. The rationale for testing the effect of EVG on the maturation and differentiation of oligodendrocytes was for several reasons. First, EVG is currently part of the front line therapy for treating HIV adults according to the latest recommendation from both the World Health Organization (WHO) and USA guidelines [9, 14]. Second, last year we reported that EVG was toxic to neurons in primary neuroglial cultures as determined by measuring the Microtubular Associated Protein 2 (MAP2) [12]. This neurotoxic effect of EVG was associated with an elevation in the level of phosphorylated eIF2α and could be reversed by an inhibitor of phosphorylated eIF2α translation attenuation [12]. Human studies show persistent white matter damage in patients with HAND, despite effective reduction of viral load in plasma. Furthermore, the white matter loss is associated with the duration of both the infection and duration of the cART. Additionally, transcriptome analysis shows alteration in myelin genes following HIV infection which continued to be dysregulated in patients who display viral suppression via cART but were diagnosed with HAND [11, 70, 74]. All of these findings lead us to question if EVG affects the ability of oligodendrocyte precursor cells to differentiation into mature oligodendrocytes. Since the literature lacked information on this

subject we started our investigation on the effect of the EVG on myelination and maturation of oligodendrocytes and its role in the development of HAND. EVG is commercially available in two different combinations. The first combination from Genvoya pharmaceutical company includes; EVG 150mg, COBI 150mg, Emtricitabine (ETC) 200mg, and Tenofovir Alafenamide (TAF) 10mg. The second choice is from Stribild pharmaceutical company EVG 150mg, COBI 150mg, ETC 200mg, and Tenofovir Disoproxil Fumarate (TDF) 300mg [9, 167]. The dose used in our *in vitro* studies was based on C_{max} plasma concentrations in patients [44]. Our lowest *in vitro* dose was one tenth of that, the middle dose was equal to the C_{max} plasma concentration and the highest dose was equal to three times the C_{max} plasma concentration [129, 168]. For the *in vivo* model, we used mass spectrometry to compare plasma levels from mice treated with EVG/COBI to plasma levels in treated patients and found mouse plasma levels comparable with those reported in human plasma (Table 4) [135].

	Time point	Average Plasma Conc. in µg/ml
C $_{max}$	4 hours	1.96
C $_{min}$	4 days	0.370

Table 4: EVG Plasma concentration in human; EVG pharmacokinetic parameters following administration of EVG/COBI , the plasma concentrations were obatained using mass spectrometry from human after administration of the drug orally (PO). N=10 [135].

These studies investigating the effects of EVG *in-vitro* and *in-vivo* provide new and compelling evidence that EVG negatively impacts oligodendrocytes

maturation. EVG impairs OPC maturation both *in-vitro* and *in-vivo*. Using stage-specific markers, EVG but not RAL inhibited the maturation of OPCs and significantly reduced the expression of MBP. This effect is mediated at the transcriptional level since our qPCR result showed a dose dependent reduction in MBP mRNA in cells treated with EVG. Interestingly, the effects of EVG are reversible at 3.5μM but not at 10μM, despite minimal cell loss at either dose. Many reasons may contribute to this observation, such as failure to remove all the EVG during the washout step or the need for a longer recovery time.

We were able to rescue OPC differentiation from the effects of EVG *in vitro* using an inhibitor of eIF2α phosphorylation translation attenuation, similar to our observations on the effects of EVG in neurons. Next, we looked at a protective cellular pathway called the integrated stress response ISR. This pathway can be activated due to a number of cellular stressors that result in the activation of one of four kinases resulting in phosphorylation of the eIF2α and global translation attenuation. In order to reverse the activation of the ISR we used a small molecule called TRANS-ISRIB to inhibit the global translation attenuation of eIF2α phosphorylatio with a dose shown to be protective in neurons [12, 169]. We found that pretreating the oligodendrocytes 1 hour prior to the treating the cells with different doses of EVG, and we found that it could protect the cells at 3.5μM but not at 10μM. More work is needed to understand the mechanisms by which 10μM EVG prevents OPC differentiation into mature oligodendrocytes.

To examine the effect of EVG *in vivo*, we used the cuprizone (bis-cyclohexanone-oxaldihydrazone) model, which is a neurotoxicant used as

model to study the demyelination and remyelination in the CNS. Cuprizone is a copper chelator that induces demyelination after 5 weeks of feeding (0.25% cuprizone mixed with normal powder food). By the end of the 5th week, gross demyelination will be observed especially in the corpus callosum (CC) with a concomitant increase in astrogliosis and microgliosis. A compensatory increase in oligodendrocyte progenitor cells will also be seen in the CC. Switching back to normal diet will result in remyelination of the CC, showing that cuprizone has a reversible effect *in vivo* [77, 140, 170]. In our experiment, we used COBI as a booster for EVG, and we tested the effect of the EVG/COBI by delivering the drug using IV cannula to the jugular vein after the 5th week of cuprizone administration to mice. To observe the effect of the drug on mature oligodendrocytes (in the mice receiving normal diet) and on immature oligodendrocytes (in the mice receiving cuprizone) and to determine if EVG/COBI will interfere with the normal remyelination process during the recovery period after cuprizone-induced demyelination. At the 5th week, we inserted IV cannulas for the administration of the drug and switched the mice back into a normal diet without cuprizone. We found that EVG/COBI attenuated normal remyelination, resulting in similar numbers of oligodendendrocytes and myelin as the group that received cuprizone in their diet for 5 weeks. The group of mice receiving cuprizone and EVG/COBI also showed an increase in GFAP positive cells, IBA1 positive cells, and NG2 positive cells as shown in Figures 11 and 12. These findings suggest an anti-inflammatory agent might protect the oligodendrocytes from the effects of EVG *in vivo*. This study gives an insight into what might be happening to oligodendrocytes in rodent models, suggesting that white matter pathologies seen in HAND may be a result from the combined effects of cART and HIV. Also, since we did not see a change in myelination when EVG/COBI was administered to control animals who had not received cuprizone, EVG/COBI may have an effect on the developing oligodednrocytes but not on the mature

oligodendrocytes, implying that EVG affects the normal turn over of new oligodendrocytes and/or remyelination after an insult. This project has a great importance in adding knowladge and clinical value for treating HIV patients with the EVG. In our analysis of the *in vivo* effects of Elvitegravir, we observed changes in myelin staining and immunofluorescence of other proteins in the CNS using immunohistochemistry [140, 172, 173]; however, due to limitations in isolation of the corpus callosum for immunoblot analysis, we were unable to validate our changes using a biochemical approach. Immunohistochemistry is widely used in basic research and for aiding in clinical diagnosis of many neurodegenerative diseases, the data obtained from these experiments is only semi-quantitative [174]. In an attempt to minimize subjectivity in our results, we have followed standard and published methods and techniques to support our interpretations [140, 172, 173]. Specifically, we used a masked observer to assign scores for myelin staining intensity combined with a computerized, automated image analysis to minimize human bias and error in the interpretation of the data.

Elvitegravir is not the only ART compound that causes white matter pathologies, we have simultaneously been investigating the mechanism of RIT mediated effects on OPC maturation. We began our studies investiagting the effect of RIT on the maturation of oligodendrocytes because we had observed previously that RIT attenuated maturation of oligodendrocyte *in vitro* but the mechanism remained undetermined [11]. Further, guidelines from WHO urge that all infected children younger than 3 years old be treated with RIT in combination with lopinavir as first line of treatment, which is a critical period for myelination [14, 171]. The dose used in my studies was qual three times the physiological concentration in the human plasma level [11]. Lipid is a major component of myelin and any disruption in the normal balance of

lipids in oligodendrocytes will result in disruption of the normal development of oligodendrocytes from the precursor stage into the mature form. Previosuly our lab published inhibiting the SREBP from entering the nucleus by using S1P inhibitor caused a significant reduction in the number of differentiated oligodendrocytes [13]. So we tested the effect of RIT on SREBP protein expression *in vitro*. Unexpectedly, we found that SREBP protein expression was increased along with the lipid enzyme FASN, both of which are responsible for the production of fatty acids. To confirm that the increase in the enzymes translated into an increase in the product, we examined the levels of palmitate and cholestoral using mass spectrometry and we found an increase of 50-60% in both the total mass of the newly synthesized palmitate and cholesterol in response to RIT. One explanation for this phenomenon could be that RIT changes the fluidity and stiffness of the oligodendrocyte membrane leading to a reduction in the differentiation of the oligodendrocytes. There may be other mechanisms at the play but this is one way in which RIT may contribute to the observations. More attention should be given to this drug especially given its recommended use for treating HIV children at critical age for myelination. In conclusion, even though ART improved the mortality and morbidity rate and overall the quality of life of HIV patients, more studies are needed to evaluate the effect of ART given to HIV-patients in CNS in general and the maturation process oligodendrocytes in particular.

Future direction:

I would like to proceed working on the effects of EVG on oligodendrocyte myelination, in the recommended treatment combinations: 1) EVG, COBI,

ETC, and TAF or 2) EVG, COBI, ETC, and TDF. The working novel model that we have developed using infusion of ART following cuprizone-induced demyelination will provide insight into the effects of compounds during the development of oligodendrocytes druing ART treatment, suggesting that this model could be used for evaluating the development of oligodendrocytes in pediatric models, during the normal turnover of the oligodendrocyte, or during injury. To reverse the effects of EVG on oligodendrocyte maturation and myelination, the literature suggests that the HIV viral protein, Tat, binds to the NMDA receptor, leading to a disruption of cytoplasmic Ca^{2+} homeostasis. Therefore, we could try blocking the effects of EVG by using an NMDA receptor inhibitor such as MK801[101]. Also, we demonstated previously that oligodendrocytes could be rescued from the effect of EVG at a 3.5 μM dose, but not at the 10 μM dose using eIF2α inhibitor TRANS-ISRIB *in vitro.* Therefore we could try attenuating the effect of EVG using TRANS-ISRIB in vivo [175]. Next, I would like to test the contribution of ART in HAND in the context of behavioral changes, brain anatomy assessed by radiographic images in the animal model. All of these tests will give us more understanding of the role of the ART in HAND.

For the role of SREBP, it is known that the majority of ART drugs cause a disturbance in lipid homeostasis in the liver [66], but limited literature has examined the effect of these drugs on oligodendrocytes despite the major role of lipids in the function of oligodendroctyes. Studying the effect of ARV on SREBP in oligodendrocytes will give us a great insight into the mechanism of development of HAND in HIV-positive patients.

Finally, I would like to use my experience in dentistry and to study the myelinated nerve axons inside the tooth pulp, since it is part of the body and linked to the CNS. Unlike other organs, the teeth are compactly innervated by primary sensory neurons found in the trigeminal ganglion, the two main nerve fibers in the teeth are A-fibers (δ- β) and C-fibers, the A fibers end in the inner one third of the dentin layer and the fibers located mainly in the pulp tissue[176, 177]. Unlike A fibers, C fibers are not myelinated and transmit the signals at much slower rate compared with A fibers[178]. Schwann cells myelinate the nerve axon in the Peripheral Nervous System (PNS), it has similar action to the oligodendrocytes in the CNS in saltatory conduction, but they have a different development and assembly of myelin, plus they do not have a cytoplasmic projection and can myelinate only one neuron axon[179]. Currently, the most common side effect from HIV in the PNS is peripheral neuropathy plus other complication, and ART did not decrease these side effects[180]. Comparing number of surfaces with caries between HIV-positive patients and un-infected patients shows that HIV patients have significantly higher number of carious surface.[181]. The mechanism behind this remains poorly understood and I would like to examine the difference between myelin proteins inside the teeth and examine the impact of HIV and ART on nerve fibers in the oral cavity.

Reference:

1.   *Human Immunodeficiency Virus (HIV).* Transfus Med Hemother, 2016. **43**(3): p. 203-22.
2.   Laskey, S.B. and R.F. Siliciano, *A mechanistic theory to explain the efficacy of antiretroviral therapy.* Nat Rev Microbiol, 2014. **12**(11): p. 772-80.
3.   Ozdener, H., *Molecular mechanisms of HIV-1 associated neurodegeneration.* J Biosci, 2005. **30**(3): p. 391-405.
4.   UNAIDS/WHO, *Global summary of the AIDS epidemic: 2009.* http://www.who.int/hiv/data/2009_global_summary.png, 2009. **Joint United Nations Programme on HIV/AIDS (UNAIDS) and World Health Organization (WHO), Geneva, Switzerland**.
5.   Kaul, M., Zheng J, Okamoto S, Gendelman HE, Lipton SA, *HIV-1 Infection and AIDS: consequences for the central nervous system.* Cell Death and Differentiation, 2005. **12**(Suppl 1): p. 878-92.
6.   Ozdener, H., *Molecular mechanisms of HIV-1 associated neurodegeneration.* J Biosci, 2005. **30**: p. 391-405.
7.   Gonzalez-Scarano, F. and J. Martin-Garcia, *The neuropathogenesis of AIDS.* Nat Rev Immunol, 2005. **5**(1): p. 69-81.
8.   Clifford, D.B., & Ances, B. M. , *HIV-Associated Neurocognitive Disorder (HAND). .* The Lancet Infectious Diseases, 2013. **13**(11): p. 976-986.
9.   AIDSINFO, *Guidelines for the Use of Antiretroviral Agents in HIV-1-Infected Adults and Adolescents.* 2018(October).
10.   Smith, R.L., et al., *Premature and accelerated aging: HIV or HAART?* Front Genet, 2012. **3**: p. 328.
11.   Jensen, B.K., et al., *Altered Oligodendrocyte Maturation and Myelin Maintenance: The Role of Antiretrovirals in HIV-Associated Neurocognitive Disorders.* J Neuropathol Exp Neurol, 2015. **74**(11): p. 1093-118.
12.   Stern, A.L., et al., *Differential Effects of Antiretroviral Drugs on Neurons In Vitro: Roles for Oxidative Stress and Integrated Stress Response.* J Neuroimmune Pharmacol, 2018. **13**(1): p. 64-76.
13.   Monnerie, H., et al., *Reduced sterol regulatory element-binding protein (SREBP) processing through site-1 protease (S1P) inhibition alters oligodendrocyte differentiation in vitro.* J Neurochem, 2016.
14.   WHO, *HIV/AIDS.* 2016(July).
15.   Chakrabarti, L., et al., *Early viral replication in the brain of SIV-infected rhesus monkeys.* Am J Pathol, 1991. **139**(6): p. 1273-80.
16.   Mankowski, J.L., et al., *Neurovirulent simian immunodeficiency virus replicates productively in endothelial cells of the central nervous system in vivo and in vitro.* J Virol, 1994. **68**(12): p. 8202-8.
17.   Argyris, E.G., et al., *Human immunodeficiency virus type 1 enters primary human brain microvascular endothelial cells by a mechanism involving cell surface proteoglycans independent of lipid rafts.* J Virol, 2003. **77**(22): p. 12140-51.
18.   Susanne Kramer-Ha ̈mmerle a, I.R.a., Horst Wolff a, Jeanne E. Bell b, Ruth Brack-Werner a, *Cells of the central nervous system as targets and reservoirs*

of the human immunodeficiency virus. Virus Research, 2005. **111**(2): p. 194-213.

19.   Esiri, M.M., C.S. Morris, and P.R. Millard, *Fate of oligodendrocytes in HIV-1 infection.* Aids, 1991. **5**(9): p. 1081-8.

20.   Li, G.H., L. Henderson, and A. Nath, *Astrocytes as an HIV Reservoir: Mechanism of HIV Infection.* Curr HIV Res, 2016. **14**(5): p. 373-381.

21.   Eugenin, E.A., et al., *Human immunodeficiency virus infection of human astrocytes disrupts blood-brain barrier integrity by a gap junction-dependent mechanism.* J Neurosci, 2011. **31**(26): p. 9456-65.

22.   O'Donnell, L.A., et al., *Human immunodeficiency virus (HIV)-induced neurotoxicity: roles for the NMDA receptor subtypes.* J Neurosci, 2006. **26**(3): p. 981-90.

23.   Antinori, A., et al., *Updated research nosology for HIV-associated neurocognitive disorders.* Neurology, 2007. **69**(18): p. 1789-99.

24.   Navia B, J.B., Price RW *The AIDS Dementia Complex: I. Clinical Features.* . Ann Neurol 1986. **19**: p. 517-524.

25.   Heaton, R., Franklin DR, Ellis RJ, McCutchan A, Letendre SL, LeBlanc S, Corkran SH, Duarte NA, Clifford DB, Woods SP, Collier AC, Marra CM, Morgello S, Mindt MR, Taylor MJ, Marcotte TD, Atkinson JH, Wolfson T, Gelman BB, McArthur JC, Simpson DM, Abramson I, Gamst A, Fennema-Notestine C, Jernigan TL, Wong J, Grant I; CHARTER Group, *HIV-associated neurocognitive disorders before and during the era of combination antiretroviral therapy: differences in rates, nature, and predictors.* J Neurovirol, 2011. **17**: p. 3-16.

26.   Gonzalez-Scarano, F., Martin-Garcia J, *The Neuropathogenesis of AIDS.* Nat Rev Immunol, 2005. **5**: p. 69-81.

27.   Brew, B., *Evidence for a change in AIDS dementia complex in the era of highly active antiretroviral therapy and the possibility of new forms of AIDS dementia complex.* AIDS, 2004. **18**(Suppl 1): p. S75-S78.

28.   Gray, F., Chretien F, Vallat-Decouvelaere AV, Scaravilli F, *The Changing Pattern of HIV Neuropathology in the HAART Era.* J Neuropathol and Exper Neurol, 2003. **62**(5): p. 429-440.

29.   Heaton, R., Clifford DB, Franklin DR, Woods SP, Ake C, Vaida F, Ellis RJ, Letendre SL, Marcotte TD, Atkinson JH, Rivera-Mindt M, Vigil OR, Taylor MJ, Collier AC, Marra CM, Gelman BB, McArthur JC, Morgello S, Simpson DM, McCutchan JA, Abramson I, Gamst A, Fennema-Notestine C, Jernigan TL, Wong J, Grant I; CHARTER Group, *HIV-associated neurocognitive disorders persist in the era of potent antiretroviral therapy.* Neurology, 2010. **75**: p. 2087-2096.

30.   Sanmarti M, I.L., Huertas S, et al., *HIV-associated neurocognitive disorders.* Journal of Molecular Psychiatry, 2014. **2**(1).

31.   Gannon, P.J., et al., *HIV Protease Inhibitors Alter Amyloid Precursor Protein Processing via beta-Site Amyloid Precursor Protein Cleaving Enzyme-1 Translational Up-Regulation.* Am J Pathol, 2017. **187**(1): p. 91-109.

32.   Broder, S., *The development of antiretroviral therapy and its impact on the HIV-1/AIDS pandemic.* Antiviral Res, 2010. **85**(1): p. 1-18.

33.   Lai, D.J., P.M. Tarwater, and R.J. Hardy, *Measuring the impact of HIV/AIDS, heart disease and malignant neoplasms on life expectancy in the USA from 1987 to 2000.* Public Health, 2006. **120**(6): p. 486-92.

34.   Teeraananchai, S., et al., *Life expectancy of HIV-positive people after starting combination antiretroviral therapy: a meta-analysis.* HIV Med, 2017. **18**(4): p. 256-266.

35.   *GLOBAL HIV STATISTICS.* 2017, UNIAIDS.

36.   El-Sadr, W.M., et al., *CD4+ count-guided interruption of antiretroviral treatment.* N Engl J Med, 2006. **355**(22): p. 2283-96.

37.   Finzi, D., et al., *Latent infection of CD4+ T cells provides a mechanism for lifelong persistence of HIV-1, even in patients on effective combination therapy.* Nat Med, 1999. **5**(5): p. 512-7.

38.   NIH, *Guidelines for the Use of AntiretroviralAgents in HIV-1-Infected Adults and Adolescents.* http://www.aidsinfo.nih.gov/contentfiles/AdultandAdolescentGL.pdf, 2011.

39.   Tilton, J.C. and R.W. Doms, *Entry inhibitors in the treatment of HIV-1 infection.* Antiviral Res, 2010. **85**(1): p. 91-100.

40.   Cihlar, T. and A.S. Ray, *Nucleoside and nucleotide HIV reverse transcriptase inhibitors: 25 years after zidovudine.* Antiviral Res, 2010. **85**(1): p. 39-58.

41.   De Clercq, E., *Non-nucleoside reverse transcriptase inhibitors (NNRTIs): past, present, and future.* Chem Biodivers, 2004. **1**(1): p. 44-64.

42.   Schafer, J.J. and K.E. Squires, *Integrase inhibitors: a novel class of antiretroviral agents.* Ann Pharmacother, 2010. **44**(1): p. 145-56.

43.   Adamson, C.S., *Protease-Mediated Maturation of HIV: Inhibitors of Protease and the Maturation Process.* Mol Biol Int, 2012. **2012**: p. 604261.

44.   Deeks, E.D., *Elvitegravir: a review of its use in adults with HIV-1 infection.* Drugs, 2014. **74**(6): p. 687-97.

45.   Tseng, A., et al., *Cobicistat Versus Ritonavir: Similar Pharmacokinetic Enhancers But Some Important Differences.* Ann Pharmacother, 2017. **51**(11): p. 1008-1022.

46.   Marzolini, C., et al., *Cobicistat versus ritonavir boosting and differences in the drug-drug interaction profiles with co-medications.* J Antimicrob Chemother, 2016. **71**(7): p. 1755-8.

47.   Varatharajan, L. and S.A. Thomas, *The transport of anti-HIV drugs across blood-CNS interfaces: summary of current knowledge and recommendations for further research.* Antiviral Res, 2009. **82**(2): p. A99-109.

48.   Hammond, E.R., et al., *The cerebrospinal fluid HIV risk score for assessing central nervous system activity in persons with HIV.* Am J Epidemiol, 2014. **180**(3): p. 297-307.

49.   Caniglia, E.C., et al., *Antiretroviral penetration into the CNS and incidence of AIDS-defining neurologic conditions.* Neurology, 2014. **83**(2): p. 134-41.

50.   Marra, C.M., et al., *Impact of combination antiretroviral therapy on cerebrospinal fluid HIV RNA and neurocognitive performance.* Aids, 2009. **23**(11): p. 1359-66.

51.   Shiu, C., et al., *HIV-1 gp120 as well as alcohol affect blood-brain barrier permeability and stress fiber formation: involvement of reactive oxygen species.* Alcohol Clin Exp Res, 2007. **31**(1): p. 130-7.

52. Ramirez, S.H., et al., *Methamphetamine disrupts blood-brain barrier function by induction of oxidative stress in brain endothelial cells.* J Cereb Blood Flow Metab, 2009. **29**(12): p. 1933-45.

53. Pakos-Zebrucka, K., et al., *The integrated stress response.* EMBO Rep, 2016. **17**(10): p. 1374-1395.

54. Zhang, K. and R.J. Kaufman, *From endoplasmic-reticulum stress to the inflammatory response.* Nature, 2008. **454**: p. 455.

55. Ron, D., *Translational control in the endoplasmic reticulum stress response.* J Clin Invest, 2002. **110**(10): p. 1383-8.

56. Korennykh, A. and P. Walter, *Structural basis of the unfolded protein response.* Annu Rev Cell Dev Biol, 2012. **28**: p. 251-77.

57. Bertolotti, A., et al., *Dynamic interaction of BiP and ER stress transducers in the unfolded-protein response.* Nat Cell Biol, 2000. **2**(6): p. 326-32.

58. Carrara, M., et al., *Noncanonical binding of BiP ATPase domain to Ire1 and Perk is dissociated by unfolded protein CH1 to initiate ER stress signaling.* Elife, 2015. **4**.

59. Vazquez de Aldana, C.R., et al., *Multicopy tRNA genes functionally suppress mutations in yeast eIF-2 alpha kinase GCN2: evidence for separate pathways coupling GCN4 expression to unchanged tRNA.* Mol Cell Biol, 1994. **14**(12): p. 7920-32.

60. Dey, M., et al., *Mechanistic link between PKR dimerization, autophosphorylation, and eIF2alpha substrate recognition.* Cell, 2005. **122**(6): p. 901-13.

61. Zhang, F., et al., *Binding of double-stranded RNA to protein kinase PKR is required for dimerization and promotes critical autophosphorylation events in the activation loop.* J Biol Chem, 2001. **276**(27): p. 24946-58.

62. Saelens, X., M. Kalai, and P. Vandenabeele, *Translation inhibition in apoptosis: caspase-dependent PKR activation and eIF2-alpha phosphorylation.* J Biol Chem, 2001. **276**(45): p. 41620-8.

63. Han, A.P., et al., *Heme-regulated eIF2alpha kinase (HRI) is required for translational regulation and survival of erythroid precursors in iron deficiency.* Embo j, 2001. **20**(23): p. 6909-18.

64. Novoa, I., et al., *Feedback inhibition of the unfolded protein response by GADD34-mediated dephosphorylation of eIF2alpha.* J Cell Biol, 2001. **153**(5): p. 1011-22.

65. Marciniak, S.J., et al., *CHOP induces death by promoting protein synthesis and oxidation in the stressed endoplasmic reticulum.* Genes Dev, 2004. **18**(24): p. 3066-77.

66. da Cunha, J., et al., *Impact of antiretroviral therapy on lipid metabolism of human immunodeficiency virus-infected patients: Old and new drugs.* World J Virol, 2015. **4**(2): p. 56-77.

67. Feeney, E.R. and P.W. Mallon, *HIV and HAART-Associated Dyslipidemia.* Open Cardiovasc Med J, 2011. **5**: p. 49-63.

68. Wohlschlaeger, J., et al., *White matter changes in HIV-1 infected brains: a combined gross anatomical and ultrastructural morphometric investigation of the corpus callosum.* Clin Neurol Neurosurg, 2009. **111**(5): p. 422-9.

69.   Gongvatana, A., et al., *White matter tract injury and cognitive impairment in human immunodeficiency virus-infected individuals.* J Neurovirol, 2009. **15**(2): p. 187-95.

70.   Tate, D.F., et al., *Regional areas and widths of the midsagittal corpus callosum among HIV-infected patients on stable antiretroviral therapies.* J Neurovirol, 2011. **17**(4): p. 368-79.

71.   Hoare, J., et al., *White matter correlates of apathy in HIV-positive subjects: a diffusion tensor imaging study.* J Neuropsychiatry Clin Neurosci, 2010. **22**(3): p. 313-20.

72.   Pomara, N., et al., *White matter abnormalities in HIV-1 infection: a diffusion tensor imaging study.* Psychiatry Res, 2001. **106**(1): p. 15-24.

73.   Ragin, A.B., et al., *Whole brain diffusion tensor imaging in HIV-associated cognitive impairment.* AJNR Am J Neuroradiol, 2004. **25**(2): p. 195-200.

74.   Borjabad, A., et al., *Significant effects of antiretroviral therapy on global gene expression in brain tissues of patients with HIV-1-associated neurocognitive disorders.* PLoS Pathog, 2011. **7**(9): p. e1002213.

75.   Organization, W.H., *Consolidated Guidelines on the Use of Antiretroviral Drugs for Treating and Preventing HIV Infection: Recommendations for a Public Health Approach*. June 2013.

76.   Wimmer, M.E., et al., *Paternal cocaine taking elicits epigenetic remodeling and memory deficits in male progeny.* Mol Psychiatry, 2017. **22**(11): p. 1641-1650.

77.   Matsushima, G.K. and P. Morell, *The neurotoxicant, cuprizone, as a model to study demyelination and remyelination in the central nervous system.* Brain Pathol, 2001. **11**(1): p. 107-16.

78.   Nickel, M. and C. Gu, *Regulation of Central Nervous System Myelination in Higher Brain Functions.* Neural Plast, 2018. **2018**: p. 6436453.

79.   Morell P, Q.R., *Characteristic Composition of Myelin.*, in *Basic Neurochemistry: Molecular, Cellular and Medical Aspects.* , A.B. Siegel GJ, Albers RW, et al, Editor. 1999, Lippincott-Raven: Philadelphia.

80.   Czopka, T., C. Ffrench-Constant, and D.A. Lyons, *Individual oligodendrocytes have only a few hours in which to generate new myelin sheaths in vivo.* Dev Cell, 2013. **25**(6): p. 599-609.

81.   Aggarwal, S., et al., *A size barrier limits protein diffusion at the cell surface to generate lipid-rich myelin-membrane sheets.* Dev Cell, 2011. **21**(3): p. 445-56.

82.   Saher, G., et al., *High cholesterol level is essential for myelin membrane growth.* Nat Neurosci, 2005. **8**(4): p. 468-75.

83.   Coetzee, T., et al., *Myelination in the absence of galactocerebroside and sulfatide: normal structure with abnormal function and regional instability.* Cell, 1996. **86**(2): p. 209-19.

84.   Yamashita, T., et al., *A vital role for glycosphingolipid synthesis during development and differentiation.* Proc Natl Acad Sci U S A, 1999. **96**(16): p. 9142-7.

85.   Ye, J. and R.A. DeBose-Boyd, *Regulation of cholesterol and fatty acid synthesis.* Cold Spring Harb Perspect Biol, 2011. **3**(7).

86.   Radhakrishnan, A., et al., *Direct binding of cholesterol to the purified membrane region of SCAP: mechanism for a sterol-sensing domain.* Mol Cell, 2004. **15**(2): p. 259-68.

87.   Brown, M.S. and J.L. Goldstein, *Cholesterol feedback: from Schoenheimer's bottle to Scap's MELADL.* J Lipid Res, 2009. **50 Suppl**(Suppl): p. S15-27.

88.   Hannah, V.C., et al., *Unsaturated fatty acids down-regulate srebp isoforms 1a and 1c by two mechanisms in HEK-293 cells.* J Biol Chem, 2001. **276**(6): p. 4365-72.

89.   Small, D.M. and G.G. Shipley, *Physical-chemical basis of lipid deposition in atherosclerosis.* Science, 1974. **185**(4147): p. 222-9.

90.   Lusis, A.J., *Atherosclerosis.* Nature, 2000. **407**(6801): p. 233-41.

91.   Chang, C.Y., D.S. Ke, and J.Y. Chen, *Essential fatty acids and human brain.* Acta Neurol Taiwan, 2009. **18**(4): p. 231-41.

92.   Keirstead, H.S. and W.F. Blakemore, *The role of oligodendrocytes and oligodendrocyte progenitors in CNS remyelination.* Adv Exp Med Biol, 1999. **468**: p. 183-97.

93.   Barateiro, A. and A. Fernandes, *Temporal oligodendrocyte lineage progression: in vitro models of proliferation, differentiation and myelination.* Biochim Biophys Acta, 2014. **1843**(9): p. 1917-29.

94.   See, J.M. and J.B. Grinspan, *Sending mixed signals: bone morphogenetic protein in myelination and demyelination.* J Neuropathol Exp Neurol, 2009. **68**(6): p. 595-604.

95.   Miller, R.H., *Regulation of oligodendrocyte development in the vertebrate CNS.* Prog Neurobiol, 2002. **67**(6): p. 451-67.

96.   Watkins, T.A., et al., *Distinct stages of myelination regulated by gamma-secretase and astrocytes in a rapidly myelinating CNS coculture system.* Neuron, 2008. **60**(4): p. 555-69.

97.   Camargo, N., et al., *Oligodendroglial myelination requires astrocyte-derived lipids.* PLoS Biol, 2017. **15**(5): p. e1002605.

98.   Waxman, S.G., *Determinants of conduction velocity in myelinated nerve fibers.* Muscle Nerve, 1980. **3**(2): p. 141-50.

99.   Miron, V.E., T. Kuhlmann, and J.P. Antel, *Cells of the oligodendroglial lineage, myelination, and remyelination.* Biochim Biophys Acta, 2011. **1812**(2): p. 184-93.

100.   Sattentau, Q.J., et al., *Epitopes of the CD4 antigen and HIV infection.* Science, 1986. **234**(4780): p. 1120-3.

101.   Zou, S., et al., *Oligodendrocytes Are Targets of HIV-1 Tat: NMDA and AMPA Receptor-Mediated Effects on Survival and Development.* J Neurosci, 2015. **35**(32): p. 11384-98.

102.   Kaul, M., et al., *HIV-1 infection and AIDS: consequences for the central nervous system.* Cell Death Differ, 2005. **12 Suppl 1**: p. 878-92.

103.   Heaton, R.K., et al., *HIV-associated neurocognitive disorders before and during the era of combination antiretroviral therapy: differences in rates, nature, and predictors.* J Neurovirol, 2011. **17**(1): p. 3-16.

104.   Saylor, D., et al., *HIV-associated neurocognitive disorder--pathogenesis and prospects for treatment.* Nat Rev Neurol, 2016. **12**(4): p. 234-48.

105. Arts, E.J. and D.J. Hazuda, *HIV-1 antiretroviral drug therapy.* Cold Spring Harb Perspect Med, 2012. **2**(4): p. a007161.

106. Saylor, D., et al., *HIV-associated neurocognitive disorder - pathogenesis and prospects for treatment.* Nat Rev Neurol, 2016.

107. Shah, A., et al., *Neurotoxicity in the Post-HAART Era: Caution for the Antiretroviral Therapeutics.* Neurotox Res, 2016. **30**(4): p. 677-697.

108. Tate, D.F., et al., *Quantitative diffusion tensor imaging tractography metrics are associated with cognitive performance among HIV-infected patients.* Brain Imaging Behav, 2010. **4**(1): p. 68-79.

109. Jernigan, T.L., et al., *Clinical factors related to brain structure in HIV: the CHARTER study.* J Neurovirol, 2011. **17**(3): p. 248-57.

110. Borjabad, A. and D.J. Volsky, *Common transcriptional signatures in brain tissue from patients with HIV-associated neurocognitive disorders, Alzheimer's disease, and Multiple Sclerosis.* J Neuroimmune Pharmacol, 2012. **7**(4): p. 914-26.

111. Bradl, M. and H. Lassmann, *Oligodendrocytes: biology and pathology.* Acta Neuropathol, 2010. **119**(1): p. 37-53.

112. McTigue, D.M. and R.B. Tripathi, *The life, death, and replacement of oligodendrocytes in the adult CNS.* J Neurochem, 2008. **107**(1): p. 1-19.

113. Lee, Y., et al., *Oligodendroglia metabolically support axons and contribute to neurodegeneration.* Nature, 2012. **487**(7408): p. 443-8.

114. Saylor, D., et al., *HIV-associated neurocognitive disorder - pathogenesis and prospects for treatment.* Nat Rev Neurol, 2016. **12**(5): p. 309.

115. Finzi, D., et al., *Identification of a reservoir for HIV-1 in patients on highly active antiretroviral therapy.* Science, 1997. **278**(5341): p. 1295-300.

116. Anthony, I.C., et al., *Influence of HAART on HIV-related CNS disease and neuroinflammation.* J Neuropathol Exp Neurol, 2005. **64**(6): p. 529-36.

117. Persidsky, Y. and L. Poluektova, *Immune privilege and HIV-1 persistence in the CNS.* Immunol Rev, 2006. **213**: p. 180-94.

118. Akay, C., et al., *Activation status of integrated stress response pathways in neurones and astrocytes of HIV-associated neurocognitive disorders (HAND) cortex.* Neuropathol Appl Neurobiol, 2012. **38**(2): p. 175-200.

119. See, J., et al., *Oligodendrocyte maturation is inhibited by bone morphogenetic protein.* Mol Cell Neurosci, 2004. **26**(4): p. 481-92.

120. Romero-Ramirez, L., M. Nieto-Sampedro, and M.A. Barreda-Manso, *Integrated Stress Response as a Therapeutic Target for CNS Injuries.* Biomed Res Int, 2017. **2017**: p. 6953156.

121. Kipp, M., et al., *The cuprizone animal model: new insights into an old story.* Acta Neuropathol, 2009. **118**(6): p. 723-36.

122. Praet, J., et al., *Cellular and molecular neuropathology of the cuprizone mouse model: clinical relevance for multiple sclerosis.* Neurosci Biobehav Rev, 2014. **47**: p. 485-505.

123. McCarthy, K.D. and J. de Vellis, *Preparation of separate astroglial and oligodendroglial cell cultures from rat cerebral tissue.* J Cell Biol, 1980. **85**(3): p. 890-902.

124. Feigenson, K., et al., *Wnt signaling is sufficient to perturb oligodendrocyte maturation.* Mol Cell Neurosci, 2009. **42**(3): p. 255-65.

125. Gavrieli, Y., Y. Sherman, and S.A. Ben-Sasson, *Identification of programmed cell death in situ via specific labeling of nuclear DNA fragmentation.* J Cell Biol, 1992. **119**(3): p. 493-501.

126. Reid, M.V., et al., *Delayed myelination in an intrauterine growth retardation model is mediated by oxidative stress upregulating bone morphogenetic protein 4.* J Neuropathol Exp Neurol, 2012. **71**(7): p. 640-53.

127. Wynn, H.E., R.C. Brundage, and C.V. Fletcher, *Clinical implications of CNS penetration of antiretroviral drugs.* CNS Drugs, 2002. **16**(9): p. 595-609.

128. Letendre, S., et al., *Validation of the CNS Penetration-Effectiveness rank for quantifying antiretroviral penetration into the central nervous system.* Arch Neurol, 2008. **65**(1): p. 65-70.

129. Podany, A.T., K.K. Scarsi, and C.V. Fletcher, *Comparative Clinical Pharmacokinetics and Pharmacodynamics of HIV-1 Integrase Strand Transfer Inhibitors.* Clin Pharmacokinet, 2017. **56**(1): p. 25-40.

130. Raff, M.C., et al., *Galactocerebroside is a specific cell-surface antigenic marker for oligodendrocytes in culture.* Nature, 1978. **274**(5673): p. 813-6.

131. Ranscht, B., et al., *Development of oligodendrocytes and Schwann cells studied with a monoclonal antibody against galactocerebroside.* Proc Natl Acad Sci U S A, 1982. **79**(8): p. 2709-13.

132. Bansal, R., et al., *Multiple and novel specificities of monoclonal antibodies O1, O4, and R-mAb used in the analysis of oligodendrocyte development.* J Neurosci Res, 1989. **24**(4): p. 548-57.

133. Baracskay, K.L., et al., *NG2-positive cells generate A2B5-positive oligodendrocyte precursor cells.* Glia, 2007. **55**(10): p. 1001-10.

134. Chari, D.M., *Remyelination in multiple sclerosis.* Int Rev Neurobiol, 2007. **79**: p. 589-620.

135. Custodio, J.M., et al., *Pharmacokinetics and safety of boosted elvitegravir in subjects with hepatic impairment.* Antimicrob Agents Chemother, 2014. **58**(5): p. 2564-9.

136. Harris, M., et al., *HIV treatment simplification to elvitegravir/cobicistat/emtricitabine/tenofovir disproxil fumarate (E/C/F/TDF) plus darunavir: a pharmacokinetic study.* AIDS Res Ther, 2017. **14**(1): p. 59.

137. Madhavarao, C.N., et al., *Immunohistochemical localization of aspartoacylase in the rat central nervous system.* J Comp Neurol, 2004. **472**(3): p. 318-29.

138. Krauspe, B.M., et al., *Short-term cuprizone feeding verifies N-acetylaspartate quantification as a marker of neurodegeneration.* J Mol Neurosci, 2015. **55**(3): p. 733-48.

139. Zhang, L., et al., *N-acetylcysteine attenuates the cuprizone-induced behavioral changes and oligodendrocyte loss in male C57BL/7 mice via its anti-inflammation actions.* J Neurosci Res, 2018. **96**(5): p. 803-816.

140. Yu, Q., et al., *Strain differences in cuprizone induced demyelination.* Cell Biosci, 2017. **7**: p. 59.

141. Lin, W., et al., *Enhanced integrated stress response promotes myelinating oligodendrocyte survival in response to interferon-gamma.* Am J Pathol, 2008. **173**(5): p. 1508-17.

142. Sidrauski, C., et al., *The small molecule ISRIB reverses the effects of eIF2alpha phosphorylation on translation and stress granule assembly.* Elife, 2015. **4**.

143. Blas-Garcia, A., et al., *Lack of mitochondrial toxicity of darunavir, raltegravir and rilpivirine in neurons and hepatocytes: a comparison with efavirenz.* J Antimicrob Chemother, 2014. **69**(11): p. 2995-3000.

144. Joseph, J., *Optimizing animal models for HIV-associated CNS dysfunction and CNS reservoir research.* Journal of NeuroVirology, 2018. **24**(2): p. 137-140.

145. Gelman, B.B., J. Endsley, and D. Kolson, *When do models of NeuroAIDS faithfully imitate "the real thing"?* J Neurovirol, 2018. **24**(2): p. 146-155.

146. Yilmaz, A., et al., *Raltegravir cerebrospinal fluid concentrations in HIV-1 infection.* PLoS One, 2009. **4**(9): p. e6877.

147. Anthonypillai, C., et al., *The distribution of the HIV protease inhibitor, ritonavir, to the brain, cerebrospinal fluid, and choroid plexuses of the guinea pig.* J Pharmacol Exp Ther, 2004. **308**(3): p. 912-20.

148. Lindl, K.A., et al., *Expression of the endoplasmic reticulum stress response marker, BiP, in the central nervous system of HIV-positive individuals.* Neuropathol Appl Neurobiol, 2007. **33**(6): p. 658-69.

149. Hussien, Y., D.R. Cavener, and B. Popko, *Genetic inactivation of PERK signaling in mouse oligodendrocytes: normal developmental myelination with increased susceptibility to inflammatory demyelination.* Glia, 2014. **62**(5): p. 680-91.

150. Way, S.W. and B. Popko, *Harnessing the integrated stress response for the treatment of multiple sclerosis.* Lancet Neurol, 2016. **15**(4): p. 434-43.

151. Taylor, L.C., et al., *17beta-estradiol protects male mice from cuprizone-induced demyelination and oligodendrocyte loss.* Neurobiol Dis, 2010. **39**(2): p. 127-37.

152. Gielen, E., et al., *Rafts in oligodendrocytes: evidence and structure-function relationship.* Glia, 2006. **54**(6): p. 499-512.

153. Goldstein, J.L., R.A. DeBose-Boyd, and M.S. Brown, *Protein sensors for membrane sterols.* Cell, 2006. **124**(1): p. 35-46.

154. Sato, R., *Sterol metabolism and SREBP activation.* Arch Biochem Biophys, 2010. **501**(2): p. 177-81.

155. Penzak, S.R. and S.K. Chuck, *Hyperlipidemia associated with HIV protease inhibitor use: pathophysiology, prevalence, risk factors and treatment.* Scand J Infect Dis, 2000. **32**(2): p. 111-23.

156. Ventura, R., et al., *Inhibition of de novo Palmitate Synthesis by Fatty Acid Synthase Induces Apoptosis in Tumor Cells by Remodeling Cell Membranes, Inhibiting Signaling Pathways, and Reprogramming Gene Expression.* EBioMedicine, 2015. **2**(8): p. 808-24.

157. Beach, J.W., *Chemotherapeutic agents for human immunodeficiency virus infection: mechanism of action, pharmacokinetics, metabolism, and adverse reactions.* Clin Ther, 1998. **20**(1): p. 2-25; discussion l.

158. AIDSINFO, *Guidelines for the Use of Antiretroviral Agents in HIV-1-Infected Adults and Adolescents.* 2016(Septmber).

159. Eagling, V.A., D.J. Back, and M.G. Barry, *Differential inhibition of cytochrome P450 isoforms by the protease inhibitors, ritonavir, saquinavir and indinavir.* Br J Clin Pharmacol, 1997. **44**(2): p. 190-4.

160. *CONSOLIDATED GUIDELINES ON THE USE OF ANTIRETROVIRAL DRUGS FOR TREATING AND PREVENTING HIV INFECTION*. 2015: World health organization.

161. Shafran, S.D., L.D. Mashinter, and S.E. Roberts, *The effect of low-dose ritonavir monotherapy on fasting serum lipid concentrations.* HIV Med, 2005. **6**(6): p. 421-5.

162. Dawaliby, R., et al., *Phosphatidylethanolamine Is a Key Regulator of Membrane Fluidity in Eukaryotic Cells.* J Biol Chem, 2016. **291**(7): p. 3658-67.

163. Palella, F.J., Delaney KM, Moorman AC, Loveless MO, Fuhrer J, Satten GA, Aschman DJ, Holmberg SD., *Declining morbidity and mortality among patients with advanced human immunodeficiency virus infection. HIV Outpatient Study Investigators.* N Engl J Med, 1998. **338**(13): p. 853-60.

164. Antinori, A., Arendt G, Becker JT, Brew BJ, Byrd DA, Cherner M, Clifford DB, Cinque P, Epstein LG, Goodkin K, Gisslen M, Grant I, Heaton RK, Joseph J, Marder K, Marra CM, McArthur JC, Nunn M, Price RW, Pulliam L, Robertston KR, Sacktor N, Valcour V, Wojna VE; , *Updated research nosology for HIV-associated neurocognitive disorders.* Neurology, 2007. **69**: p. 1789-1799.

165. Anthony, I., Ramage SN, Carnie FW, Simmonds P, Bell JE, *Influence of HAART on HIV-Related CNS Disease and Neuroinflammation.* J Neuropathol, 2005. **64**(6): p. 529-536.

166. Bhaskaran, K., Mussini C, Antinori A, Walker AS, Dorrucci M, Sabin C, Phillips A, Porter K; CASCADE Collaboration, *Changes in the Incidence and Predictors of Human Immunodeficiency Virus-Associated Dementia in the Era of Highly Active Antiretroviral Therapy.* Ann Neurol, 2007. **63**(2): p. 213-221.

167. Gunthard, H.F., et al., *Antiretroviral Drugs for Treatment and Prevention of HIV Infection in Adults: 2016 Recommendations of the International Antiviral Society-USA Panel.* Jama, 2016. **316**(2): p. 191-210.

168. Ramanathan, S., et al., *Clinical pharmacokinetic and pharmacodynamic profile of the HIV integrase inhibitor elvitegravir.* Clin Pharmacokinet, 2011. **50**(4): p. 229-44.

169. Sidrauski, C., et al., *Pharmacological brake-release of mRNA translation enhances cognitive memory.* Elife, 2013. **2**: p. e00498.

170. Polito, A. and R. Reynolds, *NG2-expressing cells as oligodendrocyte progenitors in the normal and demyelinated adult central nervous system.* J Anat, 2005. **207**(6): p. 707-16.

171. Miller, D.J., et al., *Prolonged myelination in human neocortical evolution.* Proceedings of the National Academy of Sciences, 2012. **109**(41): p. 16480.

172. Steelman, A.J., J.P. Thompson, and J. Li, *Demyelination and remyelination in anatomically distinct regions of the corpus callosum following cuprizone intoxication.* Neurosci Res, 2012. **72**(1): p. 32-42.

173. Lucchinetti, C., et al., *Heterogeneity of multiple sclerosis lesions: implications for the pathogenesis of demyelination.* Ann Neurol, 2000. **47**(6): p. 707-17.

174. Matos, L.L., et al., *Immunohistochemistry as an important tool in biomarkers detection and clinical practice.* Biomark Insights, 2010. **5**: p. 9-20.

175. Halliday, M., et al., *Partial restoration of protein synthesis rates by the small molecule ISRIB prevents neurodegeneration without pancreatic toxicity.* Cell Death Dis, 2015. **6**(3): p. e1672.

176. Fried, K., B.J. Sessle, and M. Devor, *The paradox of pain from tooth pulp: low-threshold "algoneurons"?* Pain, 2011. **152**(12): p. 2685-9.

177. Abd-Elmeguid, A. and D.C. Yu, *Dental pulp neurophysiology: part 1. Clinical and diagnostic implications.* J Can Dent Assoc, 2009. **75**(1): p. 55-9.

178. Weidner, C., et al., *Action potential conduction in the terminal arborisation of nociceptive C-fibre afferents.* J Physiol, 2003. **547**(Pt 3): p. 931-40.

179. Salzer, J.L., *Schwann cell myelination.* Cold Spring Harb Perspect Biol, 2015. **7**(8): p. a020529.

180. Ellis, R.J., et al., *Continued high prevalence and adverse clinical impact of human immunodeficiency virus-associated sensory neuropathy in the era of combination antiretroviral therapy: the CHARTER Study.* Arch Neurol, 2010. **67**(5): p. 552-8.

181. Rezaei-Soufi, L., et al., *The comparison of root caries experience between HIV-positive patients and HIV-negative individuals in a selected Iranian population.* Int J Dent Hyg, 2011. **9**(4): p. 261-5.